POLYMERIC MICROPATTERNED FILMS: A PLATFORM FOR ENHANCED MUCOADHESION

by

Yohann Aashish Pitale

B. Tech in Pharmaceutical Sciences and Technology, Institute of Chemical Technology, 2015

Submitted to the Graduate Faculty of

School of Pharmacy in partial fulfillment

of the requirements for the degree of

Master of Science

University of Pittsburgh

2017

UNIVERSITY OF PITTSBURGH

SCHOOL OF PHARMACY

This thesis was presented

by

Yohann Aashish Pitale

It was defended on

June 26, 2017

and approved by

Dr. Vinayak Sant, Assistant Professor, School of Pharmacy

Dr. Lisa Rohan, Professor, School of Pharmacy

Dr. Song Li, Professor, School of Pharmacy

Thesis Director Advisor: Dr. Vinayak Sant, Assistant Professor, School of Pharmacy

POLYMERIC MICROPATTERNED FILMS: A PLATFORM FOR ENHANCED MUCOADHESION

Yohann Aashish Pitale, B. Tech

University of Pittsburgh, 2017

Polymeric films have been established as effective mucoadhesive drug delivery systems. However, certain issues such as poor contact time with mucosal surfaces due to constant renewal of mucin need to be addressed. Current delivery systems are unable to prolong the presence of drug at the required site of action, leading to sub-optimal therapeutic activity. This work focused on designing novel micropatterned polymeric films to interact closely with the mucosa which can ultimately increase residence time of drug and reduce dosing frequency. Films of various polymer compositions were prepared using a polydimethylsiloxane mold with depressions of circle, triangle and square of specific dimensions (50, 100 and 200 μm). They were characterized for their three-dimensional (3D) morphology, mechanical properties, contact angle and mucoadhesive strength. Doxycycline hyclate was chosen as model drug to load in micropatterned films and investigate their *in vitro* release profile in conditions mimicking periodontitis. Micropatterned films were also seeded with macrophages to determine immune response the films would generate. We were able

to develop a diverse set of micropatterned films distinct in their physico-chemical properties. Micropatterns were able to significantly enhance mucoadhesion compared to plain/unpatterned films due to their higher surface area and surface roughness. Hydrophobicity offered by patterns and the presence of mucoadhesive polymer were crucial in increasing difficulty of detachment of film from mucosa. Difference in hydrophobicity of materials also governed the morphology of cells that adhered on patterned films. Dissolution studies revealed that use of pH-sensitive polymers can retard the release of DOX in disease conditions, which is essential for reducing dosing frequency and minimizing antibiotic resistance. Collectively, this work shows that 3D micropatterned films can be made using Generally Recognized as Safe (GRAS) polymers and help improve contact with mucosa for a prolonged period.

Keywords: Micropatterns, mucoadhesion, pH-sensitive, sustained release

TABLE OF CONTENTS

LIST OF TABLES

LIST OF FIGURES

PREFACE

The research work described in this MS Thesis was accomplished under the supervision of my advisor, Dr. Vinayak Sant, Department of Pharmaceutical Sciences at the University of Pittsburgh School of Pharmacy.

I sincerely thank Dr. Vinayak for guiding me through my research for two years. I am grateful to Dr. Shilpa Sant for her valuable feedback and fresh perspective. I also thank Lori Altenbaugh for administrative help she gave me throughout my Masters. I would like to acknowledge Prithivirajan Durairajan for training and helping me acquire technical skills needed for this project. I express deep gratitude for friends and Sant Lab members- Yingei Xue, Akhil Patel, Harini Krishnan, Vishal Rakshe, Manjulata Singh, and Rohita Ravindran for their assistance, critical feedback and immense support during my research.

I am also thankful to Dr. Robert Gibbs for access to Confocal Microscope and to Dr. Lisa Rohan for her encouragement and access to lab equipments.

Finally, I express deep gratitude to my parents, grandparents and sister for their care and instilling in me values needed for the completion of my studies.

1.0 INTRODUCTION

1.1 Need for Mucoadhesion

The oral route of drug delivery is an attractive route of administration owing to its convenience, lack of supervision required, rapid availability and low cost of manufacture. However, certain aspects of oral delivery may lead to sub optimal efficacy of the drug. Firstly, the acidic environment and hydrolytic enzymes in the stomach can destroy integrity of protein and other large molecules leading to oral bioavailability as low as 3% (Eaimtrakarn, Itoh et al. 2001, Chirra and Desai 2012). Secondly, conventional oral delivery may not be suitable for targeting certain local diseases due to potential systemic exposure and lack of drug permeation in required site of action within gastro-intestinal tract (GIT) (Hua, Marks et al. 2015). It is well known that reducing dosing frequency can help improve patient compliance, and lead to maximized therapeutic success (Srivastava, Arora et al. 2013). This is especially true for geriatric patients who may be on a number of medications and skip a dose accidentally (Chiang-Hanisko, Tan et al. 2014). Currently many drugs are orally administered with a high frequency, over a long period of time- this is not

feasible for costly biologics and proteins, especially for treating cancer, as most of the drug reaches healthy tissues non-specifically (Mustata and Dinh 2006).

This has set forth the need for designing novel delivery systems to address such issues so that patients get the optimal care and are not burdened by health costs.

Over the years, mucoadhesive dosage forms have generated interest in delivering small molecules and biopharmaceuticals locally as well as systemically. Mucoadhesion is defined as the state where two materials, of which at least one is the mucosa, come in close contact and stay together for a substantial amount of time due to the establishment of interfacial bonding with mucus and epithelial cell lining (Sosnik, das Neves et al. 2014) (Palacio and Bhushan 2012). Mucoadhesive drug delivery systems (MDDS) are essentially an encapsulation of Active Pharmaceutical Ingredient (API) in a polymer matrix- the polymer consists of functional groups which interact with mucus chains via various ionic and covalent bonds. MDDS offer unique advantage of targeting and localization of drug at a specific site- this allows for intimate prolonged contact with mucosa resulting in increased drug permeation at required site of action (Boddupalli, Mohammed et al. 2010) (Fox, Kim et al. 2015). MDDS are designed such that they deliver the drug at a required concentration within the therapeutic window at the right time to a specific target, in a safe and reproducible manner (Chirra and Desai 2012).

1.2 Mucus and Mucosa

Mucus is a viscoelastic adhesive gel that lines the epithelial surfaces in humans. It consists of 95% water, mucin glycoproteins-which build up structure of the gel, lipids and inorganic salts. Primarily, it serves to protect epithelial cells from pathogens, toxins, chemical and mechanical damage, and still exchange nutrients with the surrounding (Boegh and Nielsen 2015). Other functions include providing wettability and lubrication for passage of food through GIT (Boegh and Nielsen 2015) (Zhang, Shahbazi et al. 2014), maintaining homeostasis, immune-regulation and transport of sperm in cervical epithelium (Litt 1984).

Mucus is present abundantly in the body and its properties change based on their location as shown in **Table 1** (Sosnik, das Neves et al. 2014). A challenging obstacle while developing dosage forms is the continuous clearing, shedding and replenishing of mucus from the mucosal surfaces. Drug delivery scientists have to consider the mucin turnover rate of targeted site while designing dosage forms to ensure it does not slip away from mucosal lining leading to termination of therapeutic activity or even adverse reactions.

Buccal mucosa, in particular is an interesting alternative to conventional oral drug delivery. It has a moderate surface area of 50 cm^2 (Fox, Kim et al. 2015) with a rich supply of blood (Gilhotra, Ikram et al. 2014).

Table 1: Main features of different mucosal sites (Sosnik, das Neves et al. 2014)

Mucosae	Shear stress type	Mucin conc. %	pH	Clearance rate*	Mean thickness (μm)
Buccal	Resting/Mastication	0.1-0.5	6.8-7.4	0.1-1.85 mL/min	10-100
Gastric	Resting/Digesting	3	1-2.5	4-5 h	180
Small intestinal	Resting/Digesting	1	5.9-7.5	47-120 min	0-37
Rectal	Resting/Defecation	<5	6.8-7.9	3-4 h	150
Nasal	Respiration/Coughing	~2-3	6.3-6.7	5-10 min; 0.5 mL/min	10-15
Lung	Respiration/Coughing	~2-4	7	5-10 cm/min	5-55
Ocular	Blinking	0.01	7.6	5-10 s	3-5
Vaginal	Resting/Copulation	5	4.2-4.5	6 mL/d	20

Table 1 describes the changes in mucosal properties with respect to its location in the body. * Units vary as they are adapted from various references.

Proximity to neutral pH, easy accessibility (for removal in case of adverse reactions) and ability to largely bypass first pass metabolism are few of the benefits of this route. Buccal mucosa is not as permeable as sublingual mucosa and has relatively immobile mucin making it suitable for sustained release (SR)/ retentive applications (Gandhi and Robinson 1994).

Commercially available buccal products are focused on treatment of cardiovascular diseases, oral candidiasis, gingivitis, periodontitis, nausea, diabetes and migraine (Gilhotra, Ikram et al. 2014).

1.3 Micro-topographic features as a Strategy to Improve Residence Time

As mentioned earlier, there is a pressing need to prolong residence time of delivery systems to get optimum efficacy of drug. Another benefit of this is the reduction in

frequency of administration of dosage form, making patients adhere to their drug dosing regimen. There is extensive literature on use of mucoadhesive polymers or nanoparticles to improve residence of dosage forms (Szymanska, Winnicka et al. 2014, Naz, Shahnaz et al. 2017, Tejada, Barrera et al. 2017) (Majithiya, Ghosh et al. 2006) (Bilensoy, Cirpanli et al. 2007), however, this approach may have some limitations. Firstly, residence time of these systems is dependent on local mucus turnover rate (Bernkop-Schnurch 2005), so, for instance, mucoadhesive particles can remain attached to intestinal mucus only upto 4-5 h (Lai, Wang et al. 2009). Secondly, mucoadhesive systems being adhered to mucus network may not be able to transport drug to underlying epithelial cells. Studies show that premature adsorption to mucus (Lai, Wang et al. 2009) (Irache, Durrer et al. 1996) (Lehr, Bouwstra et al. 1992) can cause delivery system to be directly eliminated in feces with no therapeutic effect.

Modifying surfaces of biomaterials is an upcoming avenue in improving mucoadhesion. For instance, pills coated with micro-needles can physically penetrate epithelial tissue and increase adhesion and drug permeation (Traverso, Schoellhammer et al. 2015); and nanoengineered microparticles have shown 100 fold increase in lift off force from epithelial monolayer and 10 fold increase in *in vivo* retention, compared to unmodified microparticles (Fischer, Aleman et al. 2009). Colonoscopes are regarded as safe but at times with improper grip on mucosal tissue

can perforate colonic walls. To enhance grip, micro posts of Carbopol hydrogel were synthesized and found to have significantly higher static friction force (with colonic surface) than non-patterned mucoadhesive structures (Dodou, del Campo et al. 2007). In another work (Buselli, Pensabene et al. 2010), polydimethylsiloxane (PDMS) micro-pillars of varying diameters were coated onto legs of endoscopic capsule. Friction force and friction coefficient both showed a peak at 100 μm diameter - this enhancement, compared to flat surface is attributed to the pillars providing more space for mucus to fill up and interact better with the PDMS. Collectively, this suggests that modifying polymeric surfaces with micro-topographic features enhance friction and interaction with mucosal layer. Consequently, leading to enhanced residence time and offsetting limitations encountered in conventional oral drug delivery. This study is the first to employ rough topographic features on polymeric films to improve residence time on mucosa.

1.4 Mucosal Immune Response

Having discussed the benefits of topographic features, one must keep in mind that biomaterial surface chemistry and roughness (topographic features) can elicit immune response which further dictates i) whether a delivery system will be accepted or rejected by body and ii) what pharmacological activity will be triggered. Given that cell adhesion and interaction is complex and of growing interest in

academia and industry (Hickman, Boocock et al. 2016), this study aims to investigate effect of micropatterned polymeric films on immune cells.

Macrophages play a key role in host defense and eliminate pathogens and foreign bodies/implants by phagocytosis, macropinocytosis, clathrin- and caveolin-mediated endocytosis. They are known to actively respond to polymer, metal and ceramics (Solheim, Sudmann et al. 2000, Takebe, Champagne et al. 2003, Schutte, Xie et al. 2009). Moreover, they regulate release of cytokines, chemokines and interleukins (IL-1,6,8, TNF-α) which produce either an inflammatory or a healing effect (Lee, Stachelek et al. 2013), depending on the nature/properties of biomaterial.

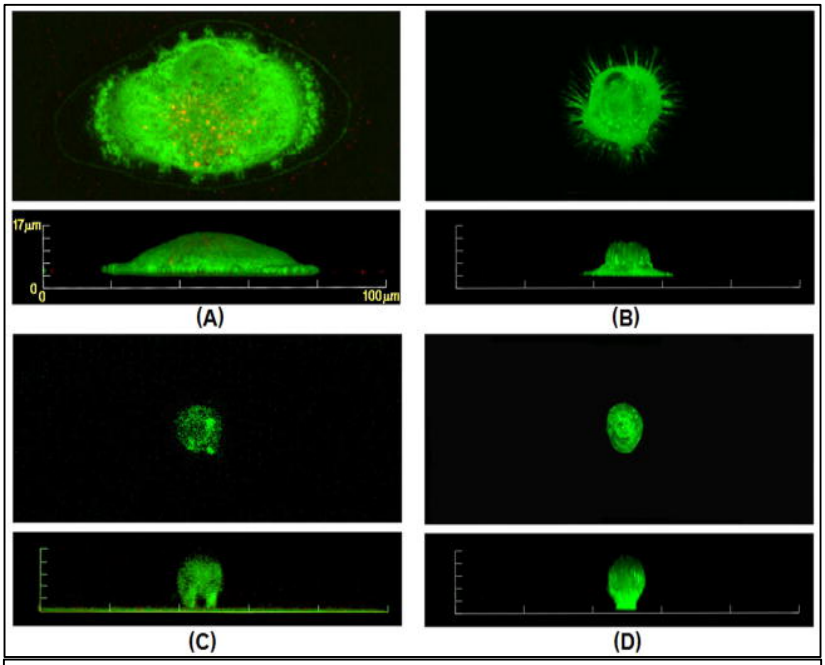

Fig 1(Lee, Stachelek et al. 2013): 3D confocal images of monocyte-derived macrophages and their distinct morphologies on (A) glass, (B) polyurethane, (C) chitosan and (D) hyaluronic acid surfaces after three days of culturing.

Surface topography is known to mediate implant-tissue reaction and influence the adhesion, differentiation and migration of cells (Hubbell, Thomas et al. 2009). Studies have shown that using a micropatterning technique, bone marrow derived macrophages were

directed into an elongated morphology and M2 polarization state (anti-inflammatory) with upregulation of M2 markers: arginase-1, CD206 AND YM-1 (McWhorter, Wang et al. 2013). Further, when elongation is attenuated, less arginase –I is produced implying impaired M2 polarization (McWhorter, Davis et al. 2015). Even the type of patterning has effect on cell morphology and phenotype. For example, micron scale patterns have shown to stimulate both pro-inflammatory (M1) as well as anti-inflammatory cytokines (M2) while nano scale patterns may not have any significant effect (Paul, Skazik et al. 2008). While cells spread abundantly, exhibiting lamellipodial extensions on glass or plastic, they may achieve hemispherical or spherical morphologies on other materials (**Fig 1(Lee, Stachelek et al. 2013)**). This can be further co-related to TNF-α secretion levels by the different biomaterials (Lee, Stachelek et al. 2013).

Hence, it is important to determine effect of biomaterials and its properties like surface chemistry and geometry among others, on the local immune system.

1.5 Periodontal Diseases

Since, this study focused on buccal mucosal application, we selected periodontal disease as our disease model to study the effectiveness of our micropatterned films. Periodontal disease is an inflammatory process involving gradual loss of the soft tissue that supports the teeth, resulting ultimately in tooth loss in susceptible patients.

A study titled “Prevalence of Periodontitis in Adults in the United States: 2009 and 2010” estimates that 47.2 percent of, or 64.7 million American adults, have mild, moderate or severe periodontitis, the more advanced form of periodontal disease. In adults 65 and older, prevalence rates increase to 70.1 percent. Higher burden of periodontitis in adult U.S population along with economic costs associated with prevention and treatment, indicate periodontitis as an important dental health problem (Eke, Dye et al. 2012).

1.5.1 pH as a factor

Variation in microbial and environmental dynamics of the oral ecosystem may increase possibility of pathogenicity and promote oral diseases. Periodontal diseases in mammals are usually associated with gram negative aerobic bacteria which colonize tooth surfaces at and below gingival margin and then proceed to destroy healthy tissue (Moore, Moore et al. 1991). Studies on the effect of pH on the growth of periodontal microorganisms showed that P. gingivalis grows at a pH of 6.5-7.0, *P. intermedia* grows at a pH of 5.0-7.0 and *F. nucleatum* grows at a pH of 5.5-7.0 (Takahashi and Schachtele 1990, Takahashi, Saito et al. 1997). One particular study advocating the use of salivary pH as a diagnostic marker in periodontal disease showed that patients with chronic generalized periodontitis had significantly lower pH than healthy volunteers (Baliga, Muglikar et al. 2013).

Buffering activity of saliva neutralizes acidity from certain foods and drinks. When one consumes sugar containing snacks regularly between meals, the pH can fall rapidly below 5 (Loesche 1996) and remain so for prolonged period of time (**Fig 2A,** (Marsh 2010)), which in turn results in colonization and enhanced growth of acid tolerant species like *lactobacilli* and *mutans streptococci*. **Fig 2B** (Marsh 2010) shows the pH range of etiologic agents of periodontitis, where most prefer acidic pH of 4 to 6 for growth. These microorganisms continue to secrete lactic acid which diffuses into the tooth and dental decay begins as Ca and PO_4 ions are released from tooth enamel (**Fig 2C**) (Loesche 1996). So clearly pH change is an important aspect in periodontal disease. However, it should be noted that there is a lack of unanimity about pH reduction. Studies like (Agha-Hosseini,

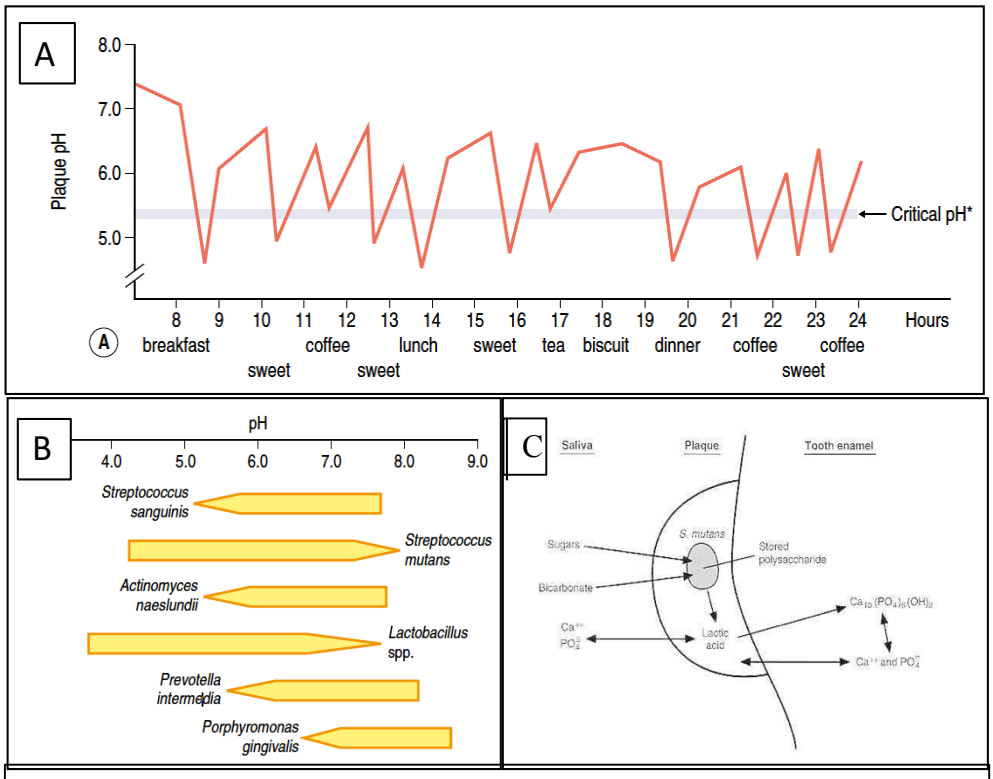

Fig 2: pH as a factor in periodontitis **A)** Time frame of pH fluctuations over course of the day (Marsh 2010) **B)** Pathogens and their optimum pH for growth (Marsh 2010) **C)** Secretion of lactic acid and dissolution of ions from enamel (Loesche 1996)

Mirzaii-Dizgah et al. 2007) (Galgut 2001) have shown that pH may actually increase or have no major change during periodontal diseases.

This study involves the use of both Sustained Release (SR) and pH-sensitive polymers to manipulate release of drug such that it releases gradually over a period of time in the periodontal disease conditions (considering lowered pH) in the gingival mucosa of buccal region.

1.5.2 Treatment Options

Eight major antibiotics used for periodontal diseases are tetracycline, minocycline, doxycycline, erythromycin, clindamycin, ampicillin, amoxicillin and metronidazole (Kapoor, Malhotra et al. 2012). In 2010, USFDA approved the use of twice daily 20 mg capsule of doxycyline hyclate (Periostat®) as an adjunct to scaling and root planning (SRP) for treatment of periodontitis. Significant reduction in probing depths, a gain in clinical attachment levels and a reduction in the incidence of disease progression worked in favor for the new product. However, limitations like development of resistant bacterial strains, emergence of opportunistic infections, gastrointestinal upset and hemorrhage due to frequent dosing, and possible allergic sensitization of patients make systemic treatment approach unsuitable. On the other hand, local treatment can help deliver drug to required site for extended period of time. Currently, ATRIDOX®, Arestin® and PerioChip® containing 10%

doxycycline hyclate, 1 mg minocycline hydrochloride and 2.5 mg chlorhexidine gluconate respectively are commercially available to treat the disease. They are composed of biodegradable polymers like PLA/PLGA or gelatin and release API in a controlled manner up to a month (Nair and Anoop 2012). Ease of application, improved results at specific site and targeting diseased sites that were not responsive to conventional therapy (Anonymous 2001) make local delivery of antibiotics an interesting opportunity to manage the disease.

1.5.3 Doxycycline hyclate

In this study, we used doxycycline hyclate (DOX) (**Fig 3**) as a model drug to load our micropatterned films with and examine its release in healthy and diseased oral conditions, specifically pH. Belonging to a class of antibiotics called tetracyclines, it is used in patients with periodontitis after SRP. Doxycycline achieves 7-20 times more concentration in gingival crevice than other drugs and has the most significant activity against *Aggregatibacter actinomycetemcomitans* which is implicated in aggressive periodontitis (Prakasam, Elavarasu et al. 2012).

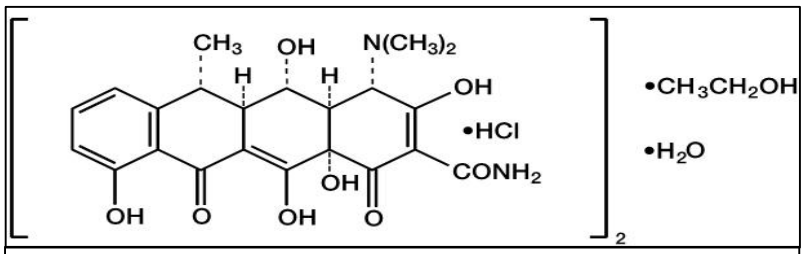

Fig 3: Chemical structure of doxycycline hyclate

In this work, we hypothesized that presence of microtopographic features on polymeric films will help in better interaction of films with mucosal surface and enhance mucoadhesion. Enhanced mucoadhesion can help film stay on mucus longer and prevent slippage. Specifically, we fabricated films with 3D pillars having circle, triangle and square patterns with defined dimensions (50, 100 or 200 μm). These films were further characterized for morphology, mechanical and surface properties. We formulated our film with pH-sensitive and SR polymers which would release drug according to the surrounding pH of periodontal disease state. Given that DOX is commercially available as twice a day capsule, we used it as a model drug and performed *in vitro* release study to show sustained release in the acidic pH which is associated with periodontal disease. We aim to show that our micropattern fabrication technique using Generally Recognized as Safe (GRAS) polymers can help the film to stay longer on mucosa and release drug slowly over time, eventually reducing dosing frequency. Finally, with the vast literature on biomaterial compatibility, we investigated the adhesion and spreading of macrophages on our micropatterned films.

2.0 MATERIAL AND METHODS

2.1 Materials

Eudragit® EPO, Eudragit® NM30 D, Eudragit® L30D 55 and plasticizer PlasACRYL™HTP20 were obtained as gift samples from Evonik Industries (Piscataway, NJ, USA). Doxycycline hyclate (DOX) was purchased from Acros Organics, (Morris Plains, NJ, USA). Hydroxy Propyl Methyl Cellulose (HPMC) E5, Triacetin and Polyethylene Glycol 400 (PEG 400) were purchased from Spectrum (New Brunswick, NJ, USA). SYLGARD® Silicone Elastomer Kit containing Elastomer Base and curing agent was procured from Dow Corning Corporation (Midland, MI, USA). Dulbecco's Modified Eagle's medium (DMEM) was purchased from Mediatech (Manassas, VA, USA).

2.2 Formulation

Since, one of the goals of this study was to engineer films which would release drug slowly according to environmental pH, we incorporated smart polymers as well as sustained release (SR) polymers in the micropatterned film. We studied three different film compositions **(Table 2, 3 and 4)** to understand the release profiles.

a) **HPMC E5-EPO (HPMC:EPO) -** HPMC is a well known water soluble release retardant polymer while cationic EPO dissolves at or below pH 5

b) **NM 30 D-EPO (NM30D:EPO) -** To further sustain drug release in neutral pH, HPMC was replaced by water insoluble SR polymer NM30D

c) **NM 30 D-L 30 D-55 (NM30D:L30D55) -** To achieve sustained release in acidic pH, EPO was replaced by anionic L30D55 which dissolves above pH 5.5

PEG 400 was used as plasticizer for hydrophilic HPMC while triacetin and PlasACRYL (emulsion of triethyl citrate and glycerol monostearate; recommended for L30D55) were used for the NM30D:EPO and NM30D:L30D55, respectively. Concentration of PEG 400 was optimized to 20% of total polymer concentration, however for compositions containing NM30D, plasticizer concentration was reduced to 10% due to the inherent good film forming and plasticizing properties of NM30D.

Table 2: Composition of HPMC:EPO film

Ingredients	**Quantity (%w/w)**		**Role**
	Film solution	**Dried film**	
HPMC E5	3.7	42.5	Sustained Release Polymer
Eudragit® EPO	3.1	35.5	pH-sensitive polymer
PEG 400	1.3	14.8	Plasticizer
Triacetin	0.63	7.2	Plasticizer
Water	91.27	-	Solvent

Table 3: Composition of NM30D:EPO film

Ingredients	Quantity (%w/w)		Role
	Film solution	Dried film	
Eudragit® EPO	3.3	43	pH-sensitive polymer
Eudragit® NM 30D	3.3	43	Sustained Release Polymer
Sodium Lauryl Sulphate (SLS)	0.4	5	Dispersing Agent/Surfactant
Triacetin	0.7	9	Plasticizer
Water	92.3	-	Solvent

Table 4: Composition of NM30D:L30D55 film

Ingredients	Quantity (%w/w)		Role
	Film solution	Dried film	
Eudragit® L30D 55	3.1	45	pH-sensitive polymer
Eudragit® NM 30D	3.1	45	Sustained Release Polymer
PlasACRYL	0.6	10	Plasticizer
Water	93.2	-	Solvent

2.3 Preparation of micropatterned films using PDMS mold

2.3.1 Fabrication of PDMS mold

Ten to one (10:1) parts by weight of Silicon Elastomer Base and Curing Agent were mixed thoroughly and air bubbles were removed under vacuum. Forty four percent of this solution known as polydimethylsiloxane (PDMS) was spread evenly on petri dish and cured at 70°C for 15 minutes to get a gel like texture. A SU-8 master template of micron sized pillars of circle, square and triangle patterns of defined dimensions (50, 100 and 200 μm) was placed on top of hardened PDMS. The remaining PDMS was poured onto the template and spread enough to cover the previous PDMS layer. This sandwiched system was further cured at 70°C for 1 hr. After curing, top PDMS layer was peeled off to remove the template and obtain the PDMS mold (negative structure of master template) with the cavities of different geometric patterns as mentioned above (**Fig 4**).

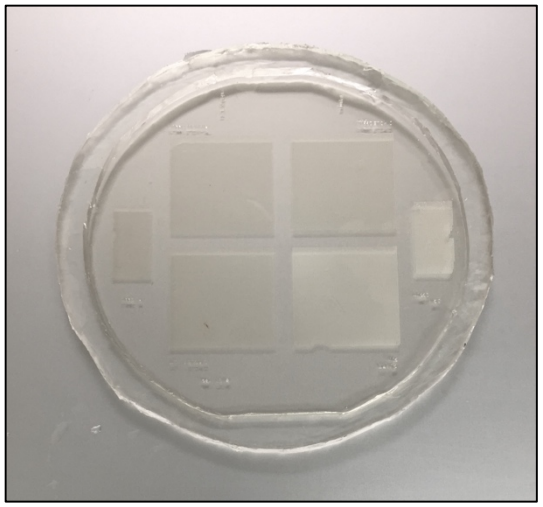

Fig 4: PDMS mold

2.3.2 Preparation of micropatterned polymeric films

Films were prepared by solvent casting technique **(Fig 5A)**, first plasticizer (depending on film composition, **Table 2/3/4**) was dissolved in MilliQ water. Then Eudragit® polymers were dispersed into solution and stirred till homogeneous. Resultant dispersion was probe sonicated for 15-20 min (Pulse mode: 4s ON, 2s OFF), following which, film solution was poured onto PDMS mold and placed under vacuum for 20-30 min till all bubbles disappeared. Lastly, film solution was dried in oven at 60-65°C overnight to obtain the micropatterned film which is a positive structure of master template **(Fig 5B)**.

In case of DOX loaded films, DOX was dissolved in water with appropriate plasticizer.

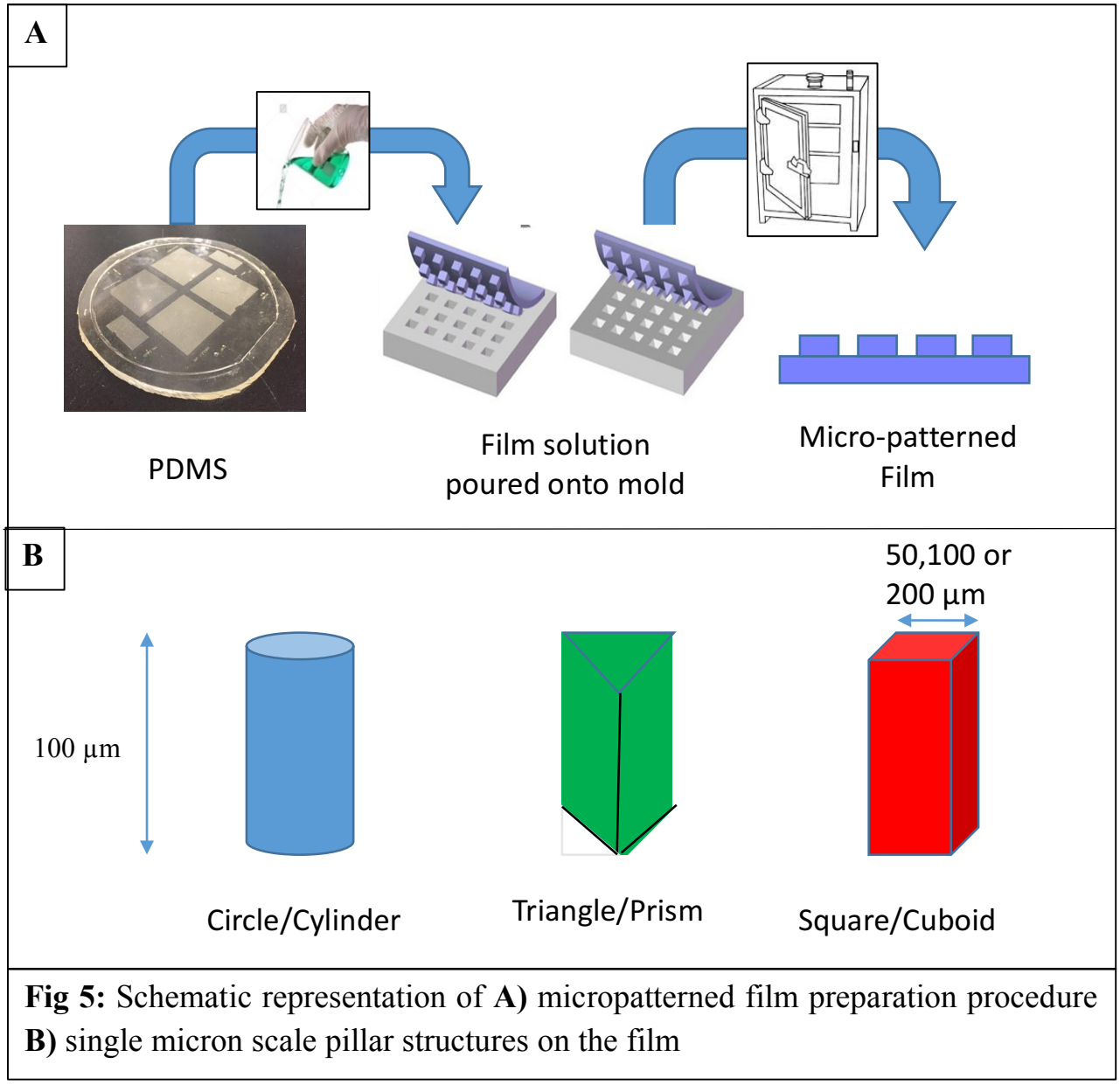

Fig 5: Schematic representation of **A)** micropatterned film preparation procedure **B)** single micron scale pillar structures on the film

2.4 Morphology and Film Thickness

After preparing films, they were sliced along an array of patterns to observe the top view and cross section of the patterned films, under light microscope (Zeiss, USA) and SEM (JEOL 9335 Field Emission SEM).

Film thickness gauge was used to measure thickness of film at 4 different points on film and the mean and % relative standard deviation (RSD) was calculated. N=4-5 films for each pattern of each composition.

2.5 Tensile Testing

Placebo film pieces of 15 X 7 mm^2 (N=6 for each pattern, taken from three separate films) were placed in between the grips of the Tensile Tester MTESTQuattro® (Norwood, MA, USA) and pulled apart at a rate of 10 mm/min till the film broke. Ultimate Tensile Strength (UTS) is the maximum force a film can bear before it breaks apart and is measured as:

$$UTS\ (MPa) = \frac{Tensile\ load\ at\ breaking\ point}{Cross\ sectional\ area}$$

Elongation denotes the change in length the film undergoes due to tensile force and is measured as:

$$\%\ elongation = \frac{(Maximum\ length\ at\ breaking\ point - original\ length)}{Original\ length} \times 100\%$$

Young's Modulus denotes the stiffness of polymer as a ratio of stress to strain experienced by film:

$$Young's\ Modulus = \frac{Tensile\ load\ at\ breaking\ point}{Cross\ sectional\ area} \div \frac{Change\ in\ length}{Original\ length}$$

2.6 *Ex vivo* Mucoadhesion Test

Porcine intestinal mucosa was excised from local slaughterhouse and preserved at -80°C. Prior to mounting on the clamp of Texture Analyzer TA.XT*Plus* (South Hamilton, MA, USA), porcine intestine tissue was thawed and cleaned thoroughly in salivary fluid simulant (SFS) and water. Films (N=6 for each pattern, taken from three separate films) were cut in circles of 8 mm diameter and taped to the TA-58 probe. A force of 150 g was applied by the probe on the mucosal tissue for 60 s and then removed from the tissue at the rate of 0.5 mm/s. After probe retrieved to its position, we obtained a) the peak detachment force (PDF) which is the maximum force needed to detach the film from tissue and b) work of adhesion which is the effort or difficulty with which the film can be separated from the mucus. Work of adhesion is essentially the area under curve of the force-distance plot obtained from Exponent software (Version 6,1,9,0).

2.7 Contact Angle

Attension Optical Tensiometer (Paramus, NJ, USA) was used to measure contact angle of the various micropatterned films. Films (N=4-5 for each pattern, taken from two separate films) were taped to a glass slide to avoid any uneven film surface due to air bubble. Eight μL of water was allowed to drop on the micropatterned film surface and mean contact angle was measured. Image was captured from the point of water droplet touching the micropatterns upto 20 s.

2.8 Weight Loss Study

Weight loss owing to dissolution of pH-sensitive polymer in the films in two pH-4.8 and 7.2 was tracked at 6, 12 and 24 h. Films (N=3 for each time point and pH) were removed from 10 mL media, lyophilized in freeze dryer, (Labconco, (Kansas City, MO, USA)) and weighed at set time points to determine % weight loss.

Images were captured from digital camera and with microscope at 10X magnification to see whether pattern dimensions are affected by the pH of media.

2.9 *In vitro* Release Study

We selected the NM30D:L30D55 film formulation to study pH-dependent release. DOX is unstable in the neutral to basic conditions (Mason, Suyemoto et al. 2011) (Wu and Fassihi 2005) provided by EPO. Hence, HPMC:EPO and NM30D:EPO were not used to show pH-dependent release of drug. Two hundred and fifty mg (250 mg) of DOX was dissolved in water before adding other excipients such that when the film formed, it had a DOX concentration of approximately 3.5 mg/cm^2. One cm^2 film was used for all drug related studies.

In vitro release of DOX from films (N=3 for each pH medium) was determined in USP Type II (Basket) Apparatus (Distek Dissolution System, Brunswick, NJ, USA). 1 x 1 cm^2 films were cut and placed in the Basket Apparatus. Fifty mL salivary fluid simulant (SFS pH 4.8) and SFS pH 7.2, maintained at 20 RPM and 37°C were used

as dissolution media to mimic periodontal disease and healthy conditions in the mouth, respectively. SFS pH 7.2 was prepared as described in (Duffo and Castillo 2004). Lactic acid, which leads to decaying of enamel *in vivo* (Loesche 1996), was used to adjust SFS pH to 4.8

Samples were collected at predetermined time intervals over 24 h, filtered, diluted (as required) and analyzed using UV/Vis Spectrophotometer at 349 nm.

2.9.1 Analytical and drug content determination

UV Standard Curve was plotted for concentrations of 0, 20, 40, 80, 100, 120, 140, 160 µg/mL in salivary fluid simulant (SFS) of pH 4.8 and 7.2, in triplicates.

Standard curve was also plotted in methanol at same concentrations to determine DOX content in the films. Briefly, 1 X 1 cm^2 sections of DOX loaded film were disrupted completely in 10 mL methanol to release all the DOX, vortexed and centrifuged at 2000 RPM for 10 min. Supernatant was filtered and diluted five times such that corresponding absorbance would lie in the middle of slope of standard curve. For above mentioned solvents λ_{max} was found to be 349 nm.

2.10 Cell Culture

J774A.1 is murine macrophage cell line, cultured in DMEM supplemented with 10% FBS (Hyclone, Utah, USA) and 1% penicillin-streptomycin (Manassas, VA, USA).

Cells were cultured in T25 and T75 flasks in a humidified incubator at 37°C and 5% CO_2. All cell culture supplies and media were obtained from Corning.

2.11 Cell Morphology

Cell studies were performed on NM30D:EPO films only. Since, L30D55 has dissolution threshold of pH 5.5, it started shedding particulate matter into the DMEM (neutral pH). These particles obscured visibility under microscope and could potentially activate cells unfavorably, hence NM30D:L30D55 was not used for this study. The smallest patterns (50 μm) of circle and square were chosen for this study, as cells were likely to respond to patterns resembling their own size.

Prior to seeding J 774A.1 (murine macrophages) on films, i) cells were cultured until they achieved 80% confluence and ii) films were cut in 8 mm diameter, placed in sterile 24 well plate (Greiner CELLSTAR®) and sterilized for 30 minutes under UV. Films were immobilized to well plate with 3 μL of polyethylene glycol dimethacrylate to prevent them from floating once media was added.

Cells were seeded at density of 150K/100 μL per film (n=2 for each pattern and each time point) in 24 well culture plates and supplemented with 300 μL fresh DMEM. Cells were incubated at 37°C: 5% CO_2 for 6 h and 24 h to study their morphology changes, spreading and association with the micropatterns. At each time point, media was removed, and adherent cells on films were fixed with 4 % paraformaldehyde for

30 min. Then cells were permeabilized in 0.1% Triton-X for 30 min, followed by staining with Hoechst (1: 1000) and Actin Green™ 488 (1 drop: 100) for 30-45 min. All stains were diluted in phosphate buffer saline (PBS) containing 0.1% Tween 20. Hoechst and Actin Green™ 488 were used to stain cells for nuclei and F-actin/cytoskeleton, respectively. After washing twice with PBS, cells were mounted on glass slide and taken for Confocal Imaging (Olympus Fluoview, Olympus). Images were taken at 10X and 40X magnification with zoom factor.

2.12 Statistical Analysis

Statistical data analysis was performed using Graph Pad Prism 6. Results are represented as Mean ± SD. Unless specified, significance between groups was analyzed using either One-way or Two-way ANOVA, followed by Tukey or Bonferroni post-hoc analysis, where necessary; a $p<0.05$ was considered significant.

3.0 RESULTS AND DISCUSSIONS

3.1. Fabrication of micro-patterned films using different polymers

Our technique was successful in fabricating thin and flexible films with height of pillar of 100 μm and pattern dimension (diameter of circle, and side of triangle, square) of 50, 100 or 200 μm. Patterns were regularly spaced all over the film and had high fidelity with respect to PDMS mold. The type of polymer used affected the film transparency slightly but all film compositions were elegant and devoid of air bubbles.

Fig. 6A and **B** show top view light microscopy and SEM images respectively, for HPMC:EPO films with 100 μm pattern posts/pillars, which confirm the formation of desired shapes with appropriate dimensions. **Fig. 6C** represents SEM images for cross-sectional view which further confirm the accurately formed height of 100 μm micro-pattern posts.

Table 5 shows the average total thickness of all formulations along with %RSD. HPMC:EPO and NM30D:EPO appear to be more uniform with respect to total film thickness. Variation in total film thickness across the formulations is due to varying amount of film solution where total solid was in the order of HPMC:EPO < NM30D:L30D55 < NM30D:EPO.

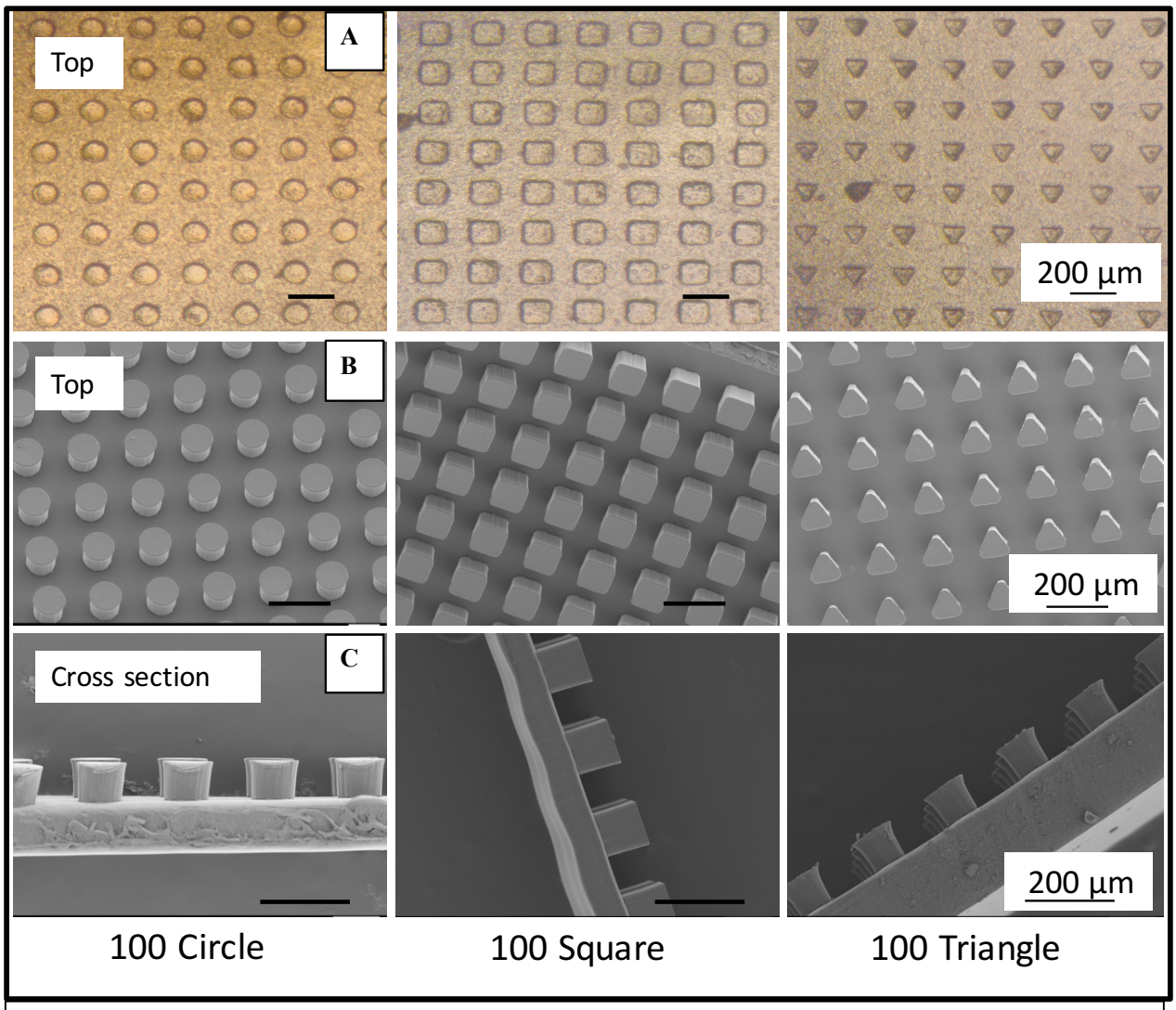

Fig 6: Morphology of HPMC-EPO micro-patterned films of 100 µm circle, square and triangle **A)** Light microscopy images of top view **B)** SEM images of top view **C)** SEM images of cross section to indicate height of posts.

Modifying polymeric film surfaces with micron sized patterns/pillars for prolonging residence time of dosage form locally is a novel concept. Presence of uniform pillars in films with three chemically different compositions shows that choice of film

forming polymer and other excipients is not a constraint for obtaining micropatterned films.

Table 5: Thickness of three film compositions calculated as Mean and %RSD, N=5.

	HPMC:EPO		NM30D:EPO		NM30D:L30D55	
	Mean (μm)	**%RSD**	**Mean (μm)**	**%RSD**	**Mean (μm)**	**%RSD**
Plain	**133**	**4.3**	**147.5**	**8.5**	**122.5**	**12.2**
100 μm Circle	**190**	**0**	**230**	**4.7**	**217.5**	**6.8**
100 μm Triangle	**203**	**5.6**	**234**	**5.7**	**230**	**7.9**
100 μm Square	**203**	**5.6**	**240**	**7.7**	**205**	**2.8**

3.2 Characterization of mechanical properties of polymeric films

After preparing micropatterned films, mechanical properties of films were studied to understand how various polymers contribute to physical strength of film. Initial studies have shown that for HPMC:EPO film composition, presence of 3D patterns on micropatterned film do not significantly impact any of the tensile properties of the film (**Fig 7 A, B**).

Then, we selected 100 μm circle and square, based on their geometry (Square has 4 sharp corners and Circle has none) and evaluated the mechanical properties across the various formulations. **Fig. 7 C, D** and **E** represent change in UTS, elongation %

and Young's Modulus as a function of polymer composition.

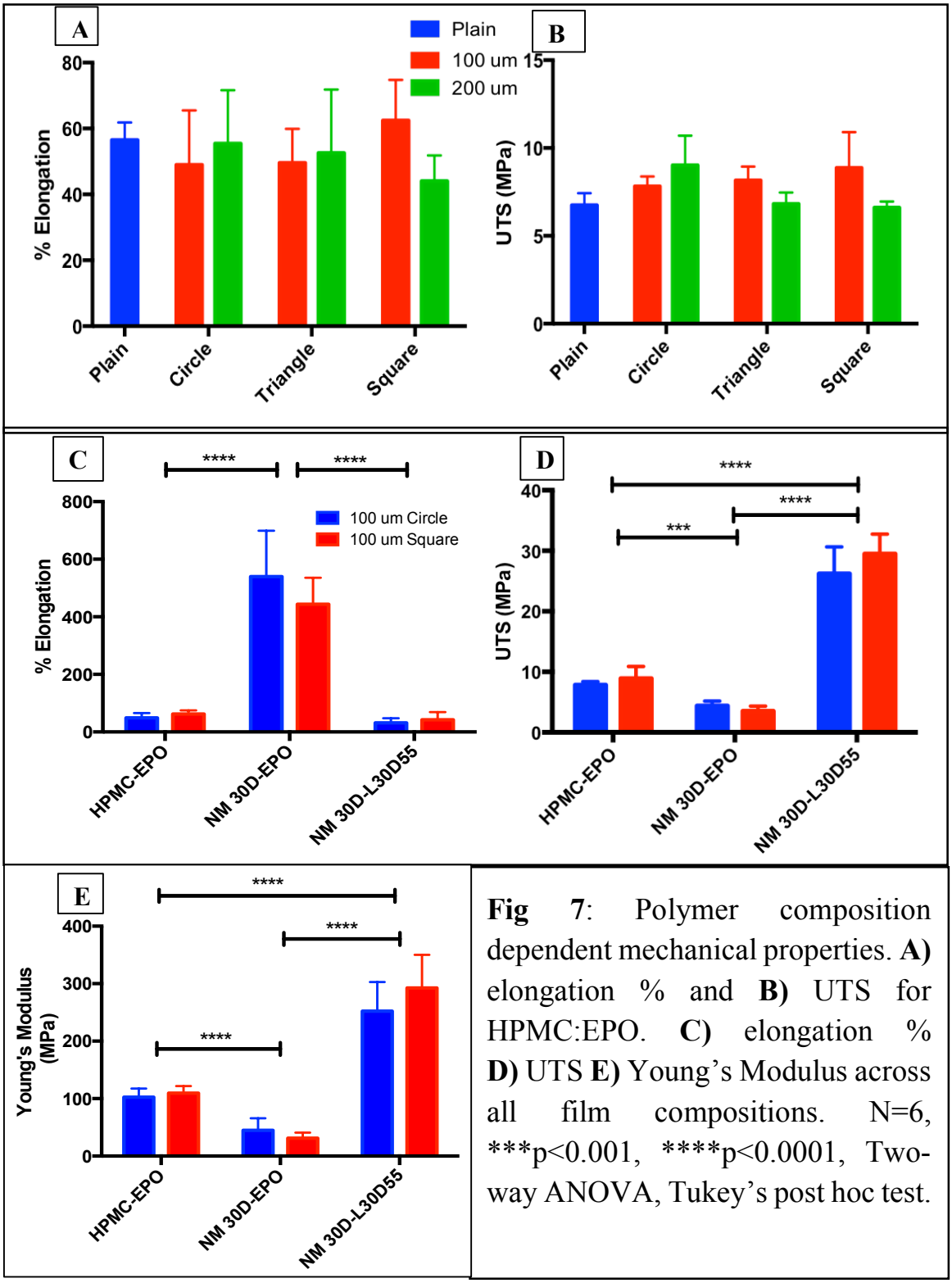

Fig 7: Polymer composition dependent mechanical properties. **A)** elongation % and **B)** UTS for HPMC:EPO. **C)** elongation % **D)** UTS **E)** Young's Modulus across all film compositions. N=6, ***p<0.001, ****p<0.0001, Two-way ANOVA, Tukey's post hoc test.

We found that the polymer chemistry has a more dominating effect on tensile properties than the microtopography of films ($p<0.001$). NM30D:EPO was very flexible and elastic as can be seen from its high elongation %. In comparison HPMC:EPO and NM30D:L30D55 films were more brittle and had to be carefully peeled out from mold after drying. Interestingly, elongation% and UTS (and Young's Modulus) have an inverse relationship as seen in other studies too (Mishra, Soni et al. 2017) (Ramineni, Cunningham et al. 2013). HPMC:EPO and NM30D:L30D55 are less ductile films (with a lower elongation) and have more tensile strength (higher UTS and Young's Modulus). A high elongation (ductility) indicates a better ability to bear stress during handling by patient while administering the film and transportation of packaged films.

3.3 Presence of micropatterns enhance mucoadhesion

There is a critical need for designing dosage forms which can stay in contact with mucosa for an extended period of time. This translates into other benefits like intimate contact of drug with mucosal surface and reduced frequency of dosing which will improve patient compliance and acceptability. We investigated whether 3D micron scale patterns can provide improved mucoadhesion over unpatterned/plain films. Our second aim was to determine which pattern shape and size is optimum for mucoadhesion.

Porcine tissue was used as it is known to closely resemble human mucosa the most (Varum, Veiga et al. 2012). We studied contact forces ranging from 50 to 200 g: lower forces did not affect mucoadhesion while higher forces like 200 g gave irreproducible results with very high variation. We selected intermediate force of 150 g, as a very large force could also harm the mucosa during application (Wong, Yuen et al. 1999). Measured outcomes were i) peak detachment force (PDF) i.e the maximum force needed to separate film from mucus layer and ii) work of adhesion i.e total work experienced by the film for detachment (Ali and Bakalis 2011). Our results did not show statistical difference for PDF (**Fig 8, first panel**) due to high standard deviations (attributed to non-uniform intestinal surface in animal). Work takes into account the extensional flow, mixing and shearing forces in the mouth (Ali and Bakalis 2011) and hence, our results are focused on work experienced by the plain and patterned films.

In all compositions, patterns (circle, triangle and square) increased work of adhesion compared to unpatterned films, showing that roughness indeed enhances friction and grip with mucosal surface (**Fig 8, second panel**). Although square patterns did not perform significantly better than other shapes, they consistently showed significantly higher work of adhesion than plain films (unlike other patterns) (**Fig 8, third panel**) and this is attributed to the highest total surface area (among all the shapes) which is able to interact with mucus; and more number of sharp corners and

edges which could possibly interpenetrate into the mucus. There is an overall trend, although not statistically significant, of triangles and squares performing better than circles- which suggests importance of sharp edges in mucoadhesion. Increasing pattern size did not influence mucoadhesion significantly except in NM 30D:L30D55 where 100 and 200 µm squares out-performed 50 µm ones.

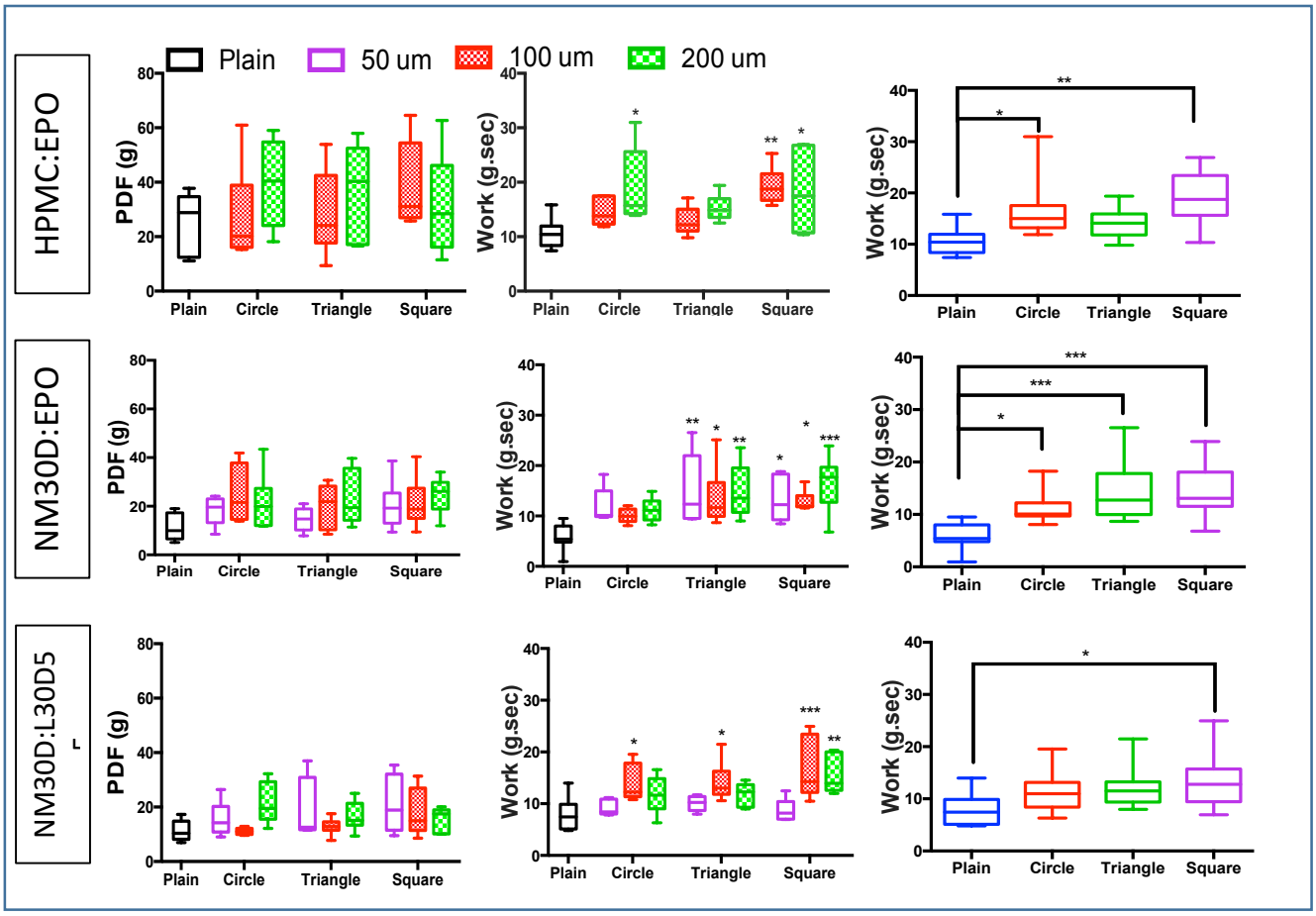

Fig 8: First panel: Peak detachment force (PDF); Second panel: work of adhesion; Third panel: Global effect of shape (irrespective of size) for HPMC:EPO, NM30D:EPO and NM30D:L30D55 *p<0.05, **p<0.01, ***p<0.001 versus Plain, One –Way ANOVA, Tukey's post hoc test.

HPMC:EPO required higher work (for all 100 μm: $p=0.0001$ versus NM30D:L30D55; for all 200 μm: $p<0.01$ versus NM30D:EPO and NM30D:L30D55) due to a combination of mucoadhesive HPMC and cationic polymer EPO which interacts with the negatively charged domains of porcine intestine (Boddupalli, Mohammed et al. 2010). When non-ionic mucoadhesive NM30D is combined with pH-sensitive polymers EPO (cationic) and L30D55 (anionic) to prepare respective films, mucoadhesion properties may not be as high as seen with typically used mucoadhesive polymers (Perioli, Ambrogi et al. 2004) (El-Kamel, Ashri et al. 2007) but they certainly achieve higher mucoadhesion than plain films. L30D55 being anionic would intuitively repel from mucin, however, its surface topography provides encouraging mucoadhesive strength. Micropatterned films allow the mucus to fill up the empty spaces between the topographic features/pillars, establishing firm contact and improving grip with tissue (Buselli, Pensabene et al. 2010)

As seen in Nature, fibrillar arrays covering feet of gecko help in maximizing interfacial adhesion of gecko (Mahdavi, Ferreira et al. 2008) with sticks and leaves- this also recapitulates our results that - presence of micro-patterns can substantially increase the difficulty of film detaching from mucosa, irrespective of the type of polymer used.

3.4 Assessing hydrophobicity of films by contact angle

Contact angles were measured to assess hydrophilicity/hydrophobicity of the different films. These help in distinguishing not only the various compositions but also the micro-patterned shapes from each other.

According to 'Lotus Effect', presence of micro-structures (trichomes and cuticular folds) on lotus leaf provide hydrophobicity making it water repellant and help in self cleansing (Yamamoto, Nishikawa et al. 2015). Further, many studies have shown that topographically modified Polyvinylidene fluoride surfaces significantly increase contact angle and this has implications on cellular responses (Paul, Skazik et al. 2008) (Lensen, Schulte et al. 2008). All film compositions showed significantly lower contact angle for plain from micropatterned films (**Fig 9 A, B** and **C** $p<0.05$) indicating that patterns increase film hydrophobicity and have better ability to hold droplet in place for longer time, than a smooth surface.

This concurs with mechanical theory of mucoadhesion that posits that surface irregularities interlock the liquid in it, increasing adhesion (Peppas and Sahlin 1996).

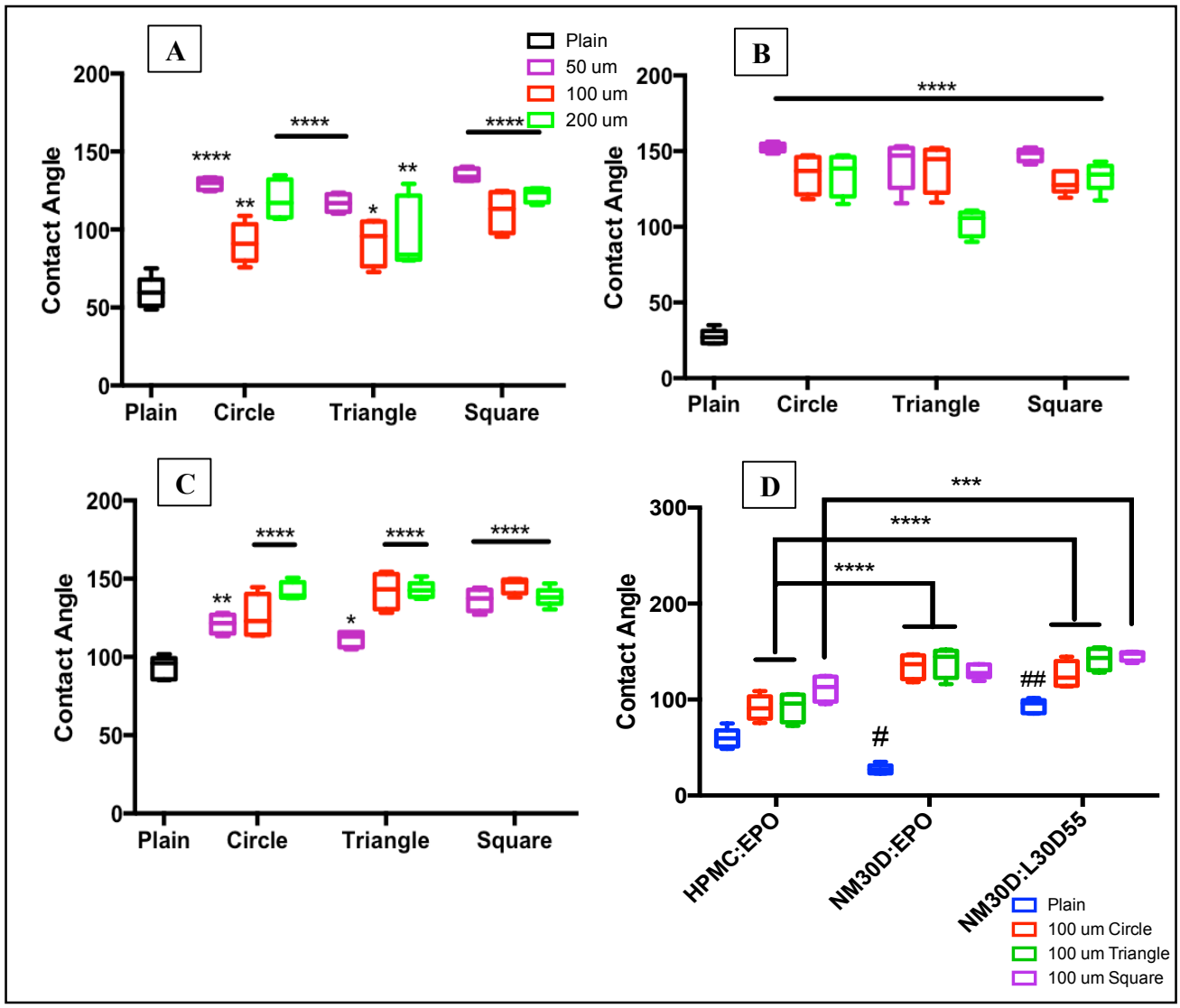

Fig 9: Contact angles quantification for **A)** HPMC:EPO **B)** NM30D:EPO **C)** NM30D:L30D55, *p<0.05, **p<0.01, **** p<0.0001 versus Plain; **D)** Comparison between compositions, #p=0.0001 versus plain of HPMC:EPO, ##p<0.0001 versus plain of HPMC:EPO, NM30D:EPO, N=5-6 One-way ANOVA, Tukey's post hoc test.

Among plain films, order of increasing hydrophobicity was NM30D:EPO < HPMC:EPO < NM30D:L30D55 (**Fig 9D,** p<0.0001). Whereas, in micropatterned films, specifically 100 µm patterns, NM30D:EPO and NM30D:L30D55 were not

statistically different from each other but had significantly higher contact angle than HPMC:EPO (**Fig 9D**, $p<0.0001$). These composition based differences are visible in **Fig 10.** Low contact angle of HPMC:EPO is due to the relatively hydrophilic components of the formulation like HPMC and PEG 400. A similar trend is seen in work of adhesion where, although not significantly, NM30D:EPO and NM30D:L30D55 behaved similarly but HPMC:EPO performed much better than other two ($p<0.01$). It appears that hydrophilic nature of HPMC:EPO augments mucoadhesive strength of this formulation. This is in accordance with Wetting theory which states that spreading of liquid onto a surface is crucial for adhesion (Smart 2005). Since NM30D:EPO had least hydrophobic plain film, it appears that surface patterning drastically increases its hydrophobicity, even surpassing that of HPMC:EPO.

Regardless of film composition and shape of micro-pattern, pattern size did not usually affect contact angle, especially in squares which were always consistent in contact angle values. Moreover, square pattern had generally higher contact angle among the patterns, and this superior ability to hold water droplet also explains higher work required by square patterns. It is important to note that not a single but a combination of theories- wetting and mechanical, contribute to mucoadhesion in this work.

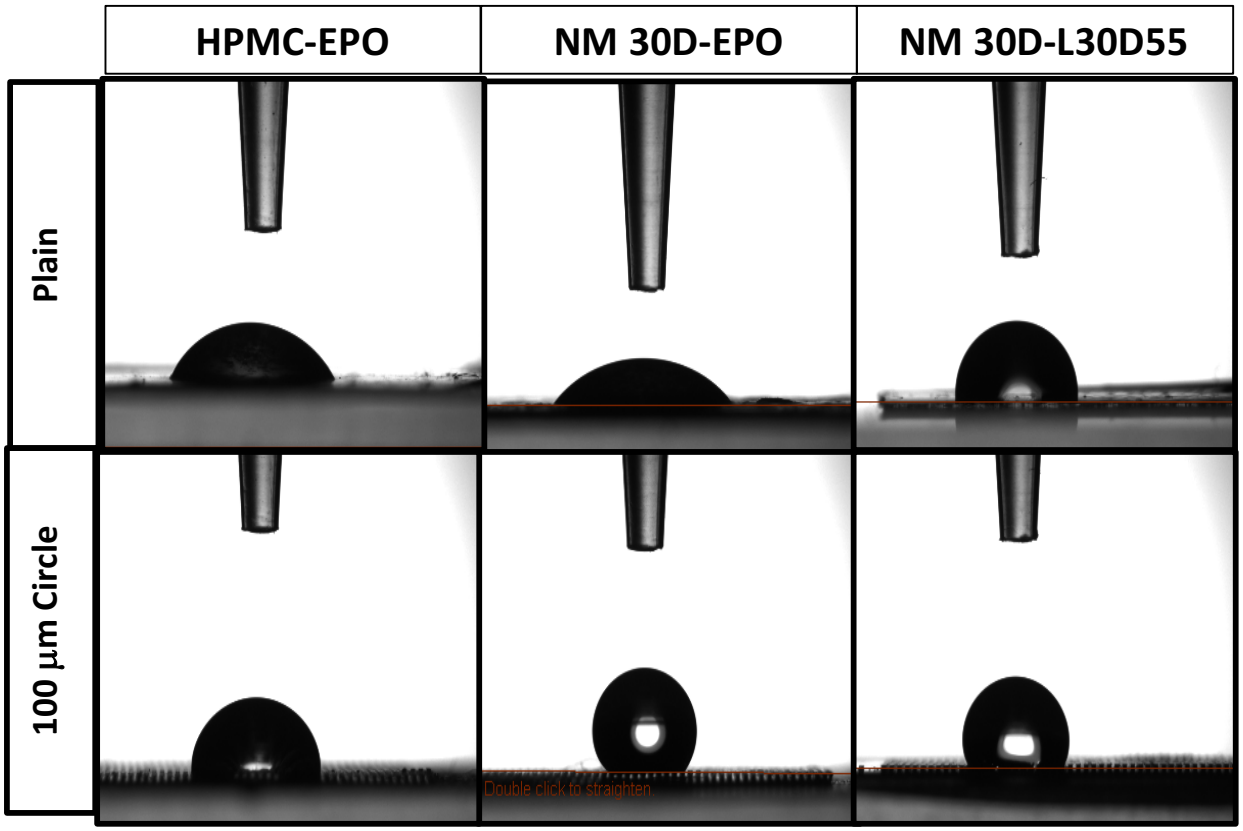

Fig 10: Contact angle images after 20 s taken from Attension goniometer for all three formulations for plain and 100 µm Circle pattern film. Extent of spreading of the droplet can be well correlated with quantified contact angle.

3.5 Films display pH dependent weight loss

Since, the goal of this study is to provide a platform for sustained release (SR) of any drug requiring pH dependent release, we performed weight loss study of placebo NM30D:EPO and NM30D:L30D55 in both physiological pHs 4.8 and 7.2. Considering the excipients of the film that would dissolve in the 2 pHs, NM30D:EPO film would be expected to have maximum weight loss of 57% (EPO, SLS and triacetin) and 14% (SLS and triacetin) in pH 4.8 and 7.2, respectively.

Similarly, NM30D:L30D55 film would be expected to have weight loss of not more than 10% (PlasACRYL) and 55% (L30D55 and PlasARYL) in low and neutral pH, respectively. In both films, observed weight loss concurred with expected weight loss (**Fig 11 A**), which implies that pH-sensitive polymer dissolves rapidly at its dissolution threshold pH, while in the other pH, it is still a part of the film and would facilitate the sustained release, if drug were to be incorporated in the film, while maintaining stability.

Fig. **11 B1** and **B2** confirm visually above findings and also that polymer loss from NM30D:L30D55 is more drastic than that from NM30D:EPO with the former film clearly shrinking in pH 7.2 while the latter film is of similar size in both pHs.

Microscopic images showed that pillars of NM30D:EPO still had dimensions proximal to 100 μm in pH 7.2 **(Fig 11 C2).** On the other hand, NM30D:L30D55 maintained its pillar dimensions in acidic pH **(Fig 11 C3)**, but were seen to reduce to 70-75 μm in neutral pH **(Fig 11 C4).** Maintaining pattern dimensions in the diseased condition of pH 4.8 (which we achieved) is crucial, as shrinking would probably lead to film loosening its mucosal grip and slip off from target site. The weight loss in the formulations was evident from macroscopic as well as microscopic images of the film.

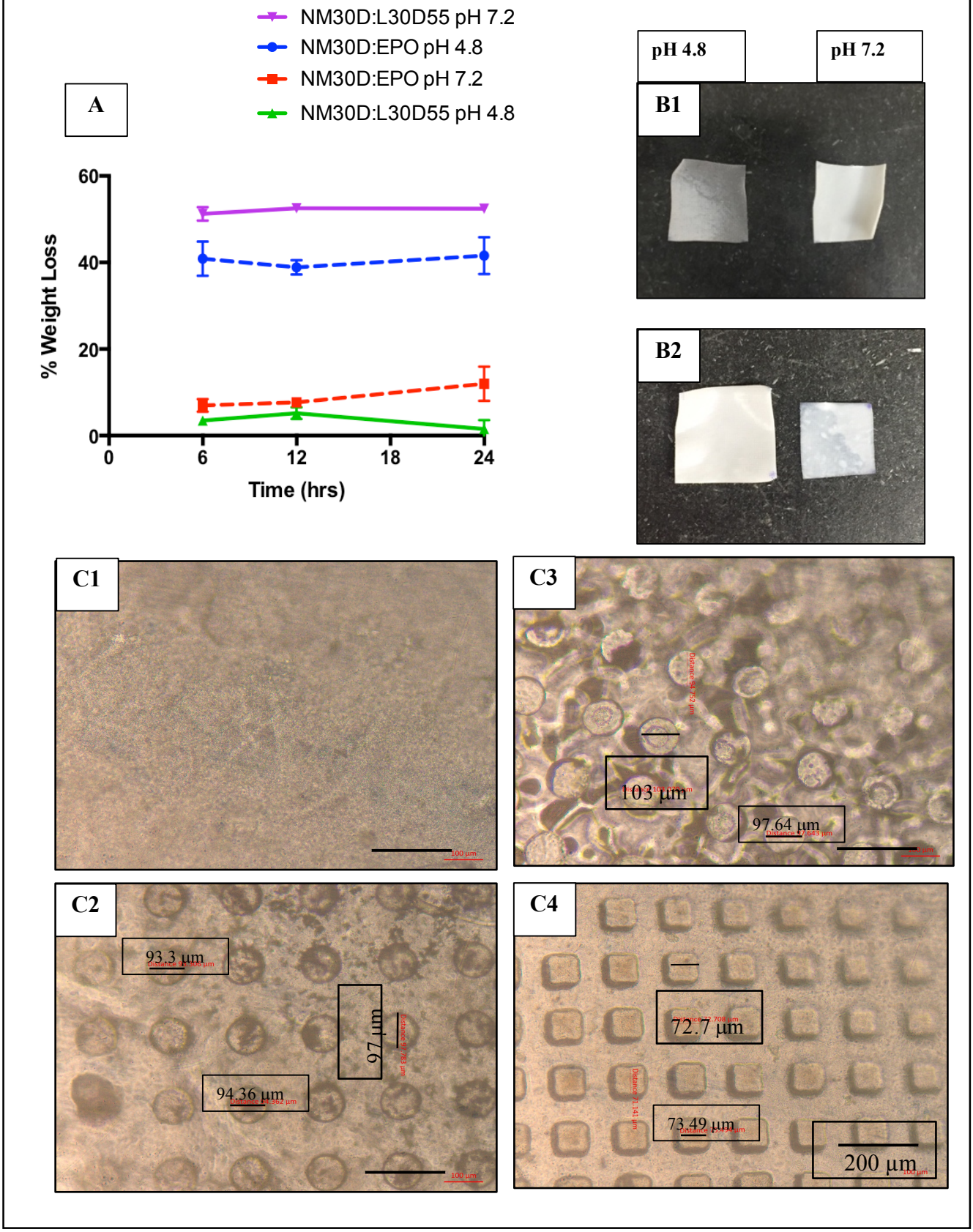
A
NM30D:L30D55 pH 7.2
NM30D:EPO pH 4.8
NM30D:EPO pH 7.2
NM30D:L30D55 pH 4.8
% Weight Loss
60
40
20
0
0
6
12
18
24
Time (hrs)
pH 4.8
pH 7.2
B1
B2
C1
C3
103 µm
97.64 µm
C2
93.3 µm
97 µm
94.36 µm
C4
72.7 µm
73.49 µm
200 µm

Fig 11: Effect of pH on weight and morphology of films **A)** Plot of % weight loss versus Time, N=3, Mean±SD; B) Visual appearance of lyophilized (**B1**) NM30D:EPO and (**B2**) NM30D:L30D55 at pH 4.8 after 24 h; (C) Post 24 h microscopy images of NM30 D:EPO in pH (**C1**) 4.8 and (**C2**)7.2 and NM30D:L30D55 in pH (**C3**) 4.8 and (**C4**) pH 7.2

3.6 Loading of DOX in micropatterned films

After establishing that both films demonstrate pH-dependent dissolution, we loaded the NM30D:L30D55 film with DOX. We selected periodontal disease, which plagues almost half the adult population of USA (Eke, Dye et al. 2012), as a model disease. As mentioned in **Section 1.5.1,** periodontitis is marked by a reduced local salivary pH (<5) and so, we used salivary fluid simulant of pH 4.8 to mimic disease condition and pH 7.2 to mimic healthy oral environment. DOX is the API present in FDA approved Periostat® capsules for this disease, so we selected DOX as a model drug to load our films and track its release in different pH.

3.6.1 Standard curves

Fig 12 show standard curves for DOX in 3 different media. Standard curves in **Fig 12 A** and **B** were used to measure concentration of drug release in pH 4.8 and 7.2, respectively. Standard curve in **Fig 12 C** was used to measure drug content in film and residual drug remaining in film after *in vitro* release. All standard curves had $R^2 > 0.99$.

Loading efficiency (%) (**Fig 12 D**) was used for calculating drug cumulative release% during *in vitro* release studies. Both patterned films achieved more than 80% loading efficiency implying that DOX can be encapsulated in NM30D:L30D55 films. When calculated as % weight of film, films had a loading of 14.85 ± 2.64 mg DOX in 100 mg of film, that corresponds to approximately 7 mg in 1 X 2 cm^2 film (**Section 2.9**) which would be applied to the gingiva. Since, the aim of this work was to show pH dependent release of the drug, we loaded our films with a model dose (3.5 mg/cm^2 of film) yet mimicked the therapeutic dose as closely as possible. Clinically, ATRIDOX® provides controlled release of 50 mg DOX over 7 days, assuming uniform release, 7.14 mg DOX is released per day- which closely matches with our dosing of NM30D:L30D55 films. Future studies will involve improving loading efficiency and checking stability of DOX in the film.

3.6.2 L30D55 prolongs release of DOX in periodontal disease mimetic conditions

As mentioned in **Section 2.9**, NM30D:L30D55 was selected to perform in vitro release studies due to incompatibility of EPO with DOX in other two formulations. EPO provides a basic pH (6.5) to film solution- this basic environment leads to formation of degradant isotetracycline (Mohammed-Ali, 2012) which possibly gives the film a brown color. To investigate whether the combination of SR and pH-

sensitive polymer would modulate DOX release in acidic and neutral pH, cumulative release % released from NM30D:L30D55 (film solution of pH 2-3) was plotted as a function of time. DOX being highly water soluble achieved more than 20% release in first 5 minutes in both media. However, at later time points, more than 60% DOX had released in 2 h due to dissolution of L30D55 in its threshold pH 7.2; while at pH 4.8, L30D55 did not dissolve as quickly: releasing less than 40% DOX in same 2h (**Fig 13 A**).

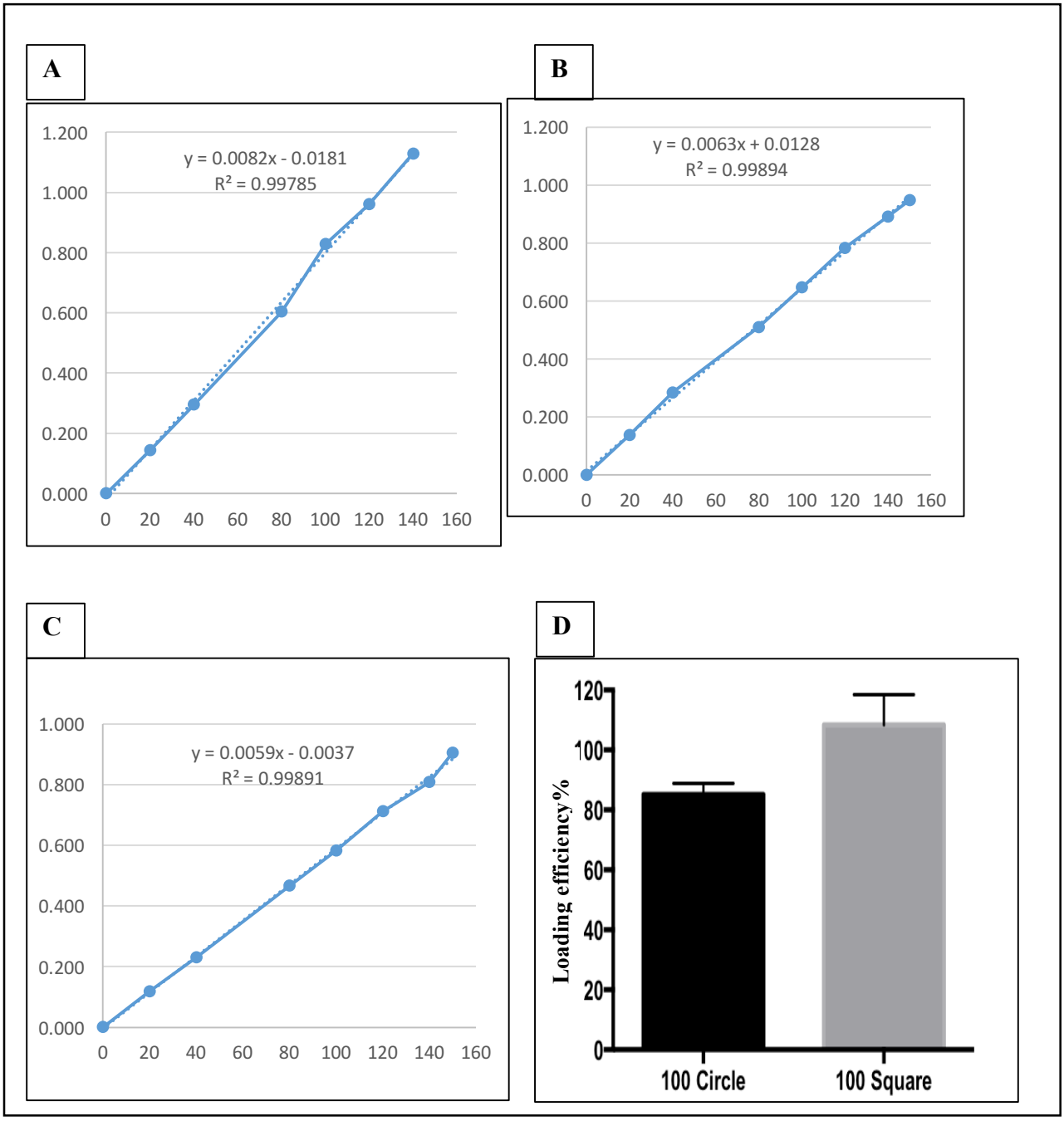
A
y = 0.0082x - 0.0181
R² = 0.99785
B
y = 0.0063x + 0.0128
R² = 0.99894
C
y = 0.0059x - 0.0037
R² = 0.99891
D
Loading efficiency%
100 Circle
100 Square

Fig 12: DOX Calibration curves performed in **A)** pH 4.8 **B)** pH 7.2 **C)** Methanol by UV-Visible Spectroscopy at 349 nm for all solvents. N=3 and **D)** Drug loading efficiency % as determined in methanol.

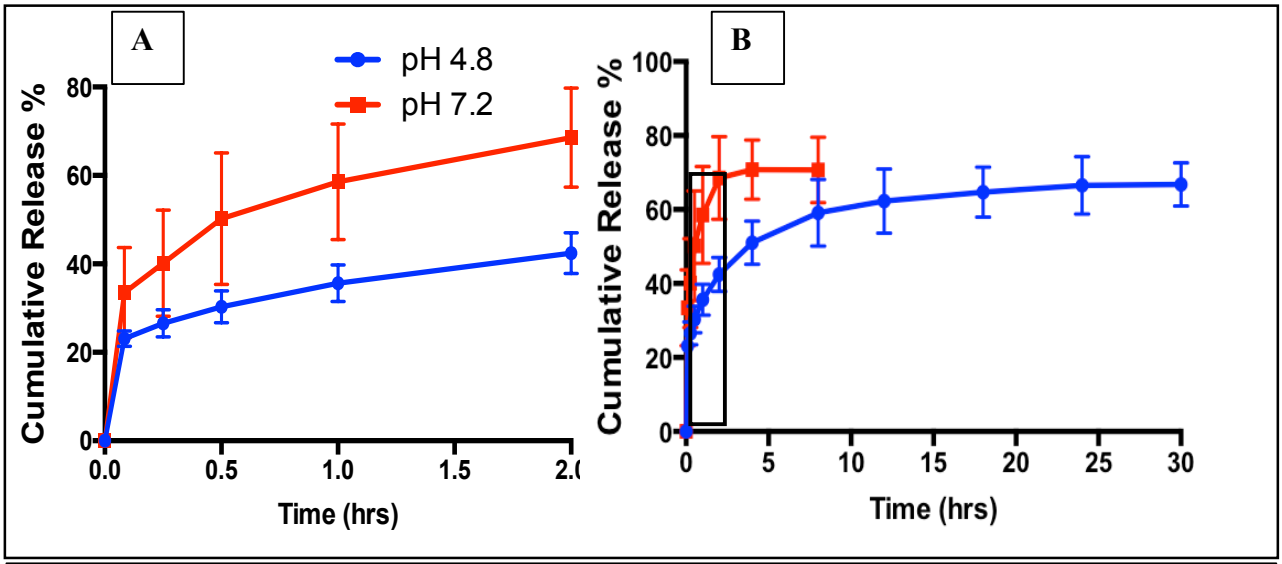

Fig 13: Release behavior of DOX from NM30D:L30D55 film in pH 4.8 and 7.2 up to **A)** 2 h [Inset of **B**] and **B)** end of study. Cumulative release represented as Mean ± SD (N=6).

This suggests a biphasic release of the drug in pH 4.8 where a burst release is seen in the first 30 min and then the release delays over 24 h. Thus, NM30D:L30D55 film retained the DOX in its polymer matrix and the managed SR up to 12 h and then began to plateau, while in pH 7.2 DOX reached its peak concentration in only 4h (**Fig 13 B**). As mentioned in **Section 1.5.1**, Periodontitis is marked with a reduced

local oral pH; NM30D:L30D55 film will release DOX relatively at a slower rate in disease condition pH 4.8. Liquids and gels administered sub-gingivally do not have satisfactorily prolonged release, also immediate clearance of drug from periodontal environment due increased flow rate of gingival crevicular fluid (GCF) is an obstacle for attaining desired efficacy (Bromberg, Braman et al. 2000). Presence of micropatterns on film can interact intimately with gingival mucosa eliminating this concern. Compared to Periostat® and other systemic approaches of treatment (Kapoor, Malhotra et al. 2012) (Slots, Research et al. 2004), this mucoadhesive sustained release delivery system could help limit drug for longer time, only to target site that is at or near the periodontal pockets (Da Rocha, Silva et al. 2015).

Moreover, current antimicrobial therapies like ATRIDOX® and Arestin® require a syringe, while PerioChip® requires to be administered by dental hygienist in a clinical setting. NM30D:L30D55 film, as adjuvant therapy with SRP, would require to be simply applied to gingival mucosa by patient himself prior to, or after SRP.

Collectively, data suggests that appropriate combination of polymers can provide immediate or sustained release in a given diseased state. NM30D:EPO would be beneficial in diseases like Bacterial Vaginosis or Vaginal atrophy where vaginal pH exceeds 4-5 due to elimination of healthy Lactobacilli (Wilson 2004, Koumans, Sternberg et al. 2007). EPO would disperse slowly in the elevated pH and provide SR.

3.7 Cell spreading influenced by surface material and time

Modulation of biomaterial properties like surface wettability, roughness, surface chemistry, stiffness and geometry have been known to influence cell and material interaction. It is necessary to understand whether micropatterns can affect immune response and whether these films would have a detrimental effect to patient (like heightened immune activation and fibrosis) after administration of film. We quantified spreading of J774A.1 macrophages on 50 μm size patterned NM30D:EPO films due to shedding of L30D55 in DMEM, which obscured cell visualization (**Section 2.11**).

Macrophages adhered to polystyrene/plastic surface of well plate as well as the polymeric film. However, cells preferred the plastic to the film, as few hours after seeding cell density was higher on plastic, suggesting that over time, cells migrated from the film to the surrounding plastic surface in the well plate. At both time points, cells spreading was significantly higher on the plastic ($p<0.0001$) while no differences were seen among the plain and micropatterned films (**Fig 14, 15**).

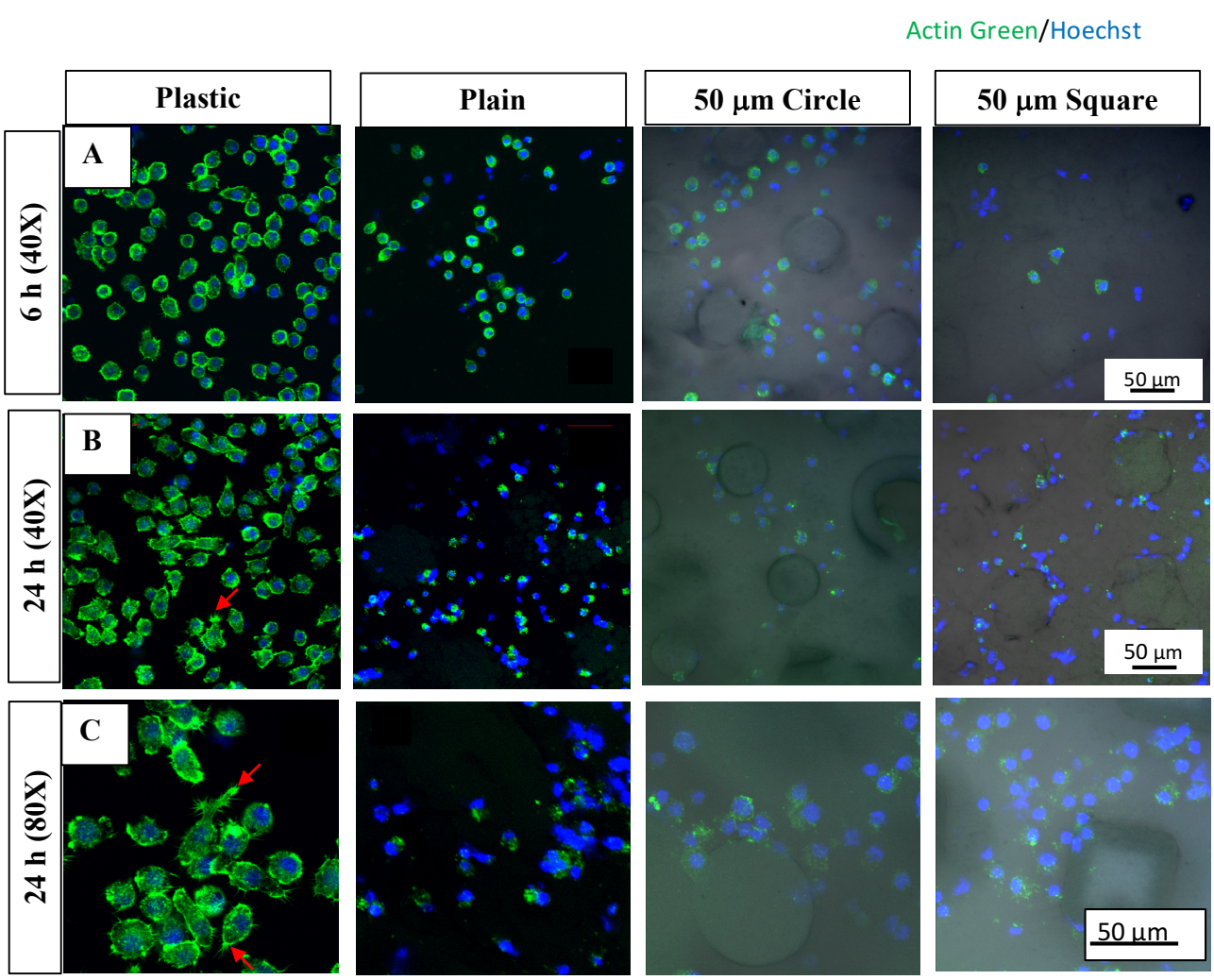

Fig 14: Cell morphology influenced by material surface, microtopography (horizontal panels) and time (vertical panels). Macrophages on plastic (polystyrene culture plate), plain, 50 µm circle and 50 µm square patterned film at **A)** 6h Low magnification **B)** 24 h, with significantly reduced average cell area Low magnification **C)** 24 h High magnification (red arrows indicating ruffles).

Molecular architecture like macrophage ruffles and filopodial projections were distinctly seen on plastic (red arrows on **Fig 14 B** and **C**) while cells on film appeared

to be more rounded in morphology with few or almost no ruffles on the cell periphery. One reason is the difference in contact angle between materials. Tissue culture polystyrene has contact angle of ~ 77° which is within optimum range for cell adhesion i.e between 55° and 85° (Lensen, Schulte et al. 2008), while our studies (**Section 3.4**) showed that NM30D:EPO plain and patterned films have contact angle of 27° and 140°, respectively. Materials having contact angle beyond the optimum range (too hydrophilic or hydrophobic) are known to cause decreased cell adhesion (Dowling, Miller et al. 2011) (Lensen, Schulte et al. 2008). Secondly, stiffer substrates (quantified by Young's Modulus) can affect the alignment of F-actin structures, increasing actin polymerization and filopodial projections (McWhorter, Davis et al. 2015) (Fereol, Fodil et al. 2006) (Patel, Bole et al. 2012). Young's Modulus for polystyrene is 3000 MPa (Prasad, Kopycinska et al. 2002) while the same for NM30D:EPO film is 50 MPa (**Fig 7E**) indicating that the film is less rigid. The difference in cell spreading and actin polymerization between plastic and NM30D:EPO film is congruent to study showing increased actin staining, membrane extensions and macrophage ruffles when cells were cultured on more rigid (150 kPa) than softer (1.2 kPa) substrates (Patel, Bole et al. 2012). Since there was no significant difference in Young's Modulus between plain and patterned films, there was similarly no difference in the spreading, adhesion and presence of macrophage extensions among the plain, circle and square patterned films. Clearly, material

surface properties, wettability, microtopography and intracellular mechanics influenced cell adhesion and spreading/morphology of macrophages.

In spite of grooves, ridges and troughs being known to guide cells to elongate (McWhorter, Wang et al. 2013) (Chen, Jones et al. 2010), square and circle patterns on film did not affect cell morphology from plain film or between each other. This is possibly due to the relatively large size of post structures- most studies use gratings of up to a few microns. In fact, polymeric microspheres for vaccine delivery are designed to be of 2-3 μm so they can get uptaken by macrophages (Champion, Walker et al. 2008). In our films, distance between two posts is 100 μm which is too wide to instruct the cells to elongate.

As expected, cells spread even more at 24 h on plastic ($p<0.01$). Surprisingly, plain film ($p<0.0001$), square ($p<0.001$) and circle ($p=0.09$) patterned films showed a reduction in average cell area (**Fig 15**). Cells remained in the rounded morphology, which may indicate acquiring an M1 polarization state (McWhorter, Davis et al. 2015) that could be required for engulfing the various microflora implicated in periodontitis. Rounded morphology of cells is not unusual as polyurethane (Lee, Stachelek et al. 2013) (Stachelek, Finley et al. 2011), chitosan and hyaluronic acid (Lee, Stachelek et al. 2013) have been reported to give rise to such shapes of adherent macrophages.

Regarding location of the cells on the film, the majority of them were found on the flat base of micropatterned films. While the ones associated with the posts, were found attached more to the periphery than the face of the posts (red arrows on **Fig. 16 A, B**).

As described in **Section 1.4**, cell shape and cytokine secretion/immune response can be well correlated. In spite of our results on morphology differences, we cannot infer the polarization state achieved by the macrophages and therefore, it is crucial to investigate regulation of pro-inflammatory and anti-inflammatory markers and then establish a relationship between morphologies as seen on the film and plastic surface.

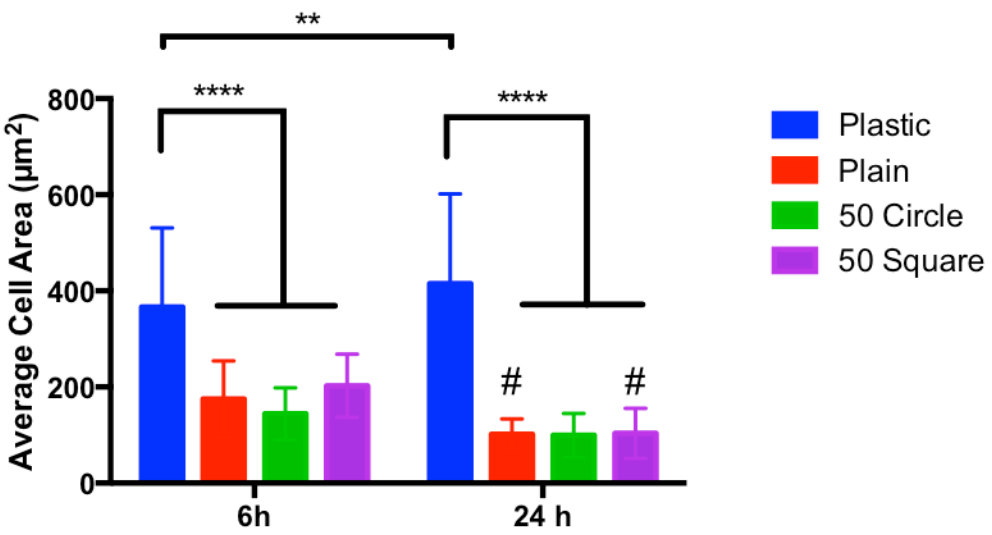

Fig 15: Cell area quantification of micropatterned films versus Time. N= 2 films for each pattern and time point. #p<0.001 versus corresponding 6 h time point, **p<0.01, **p<0.0001Two Way ANOVA, Bonferonni's Test.

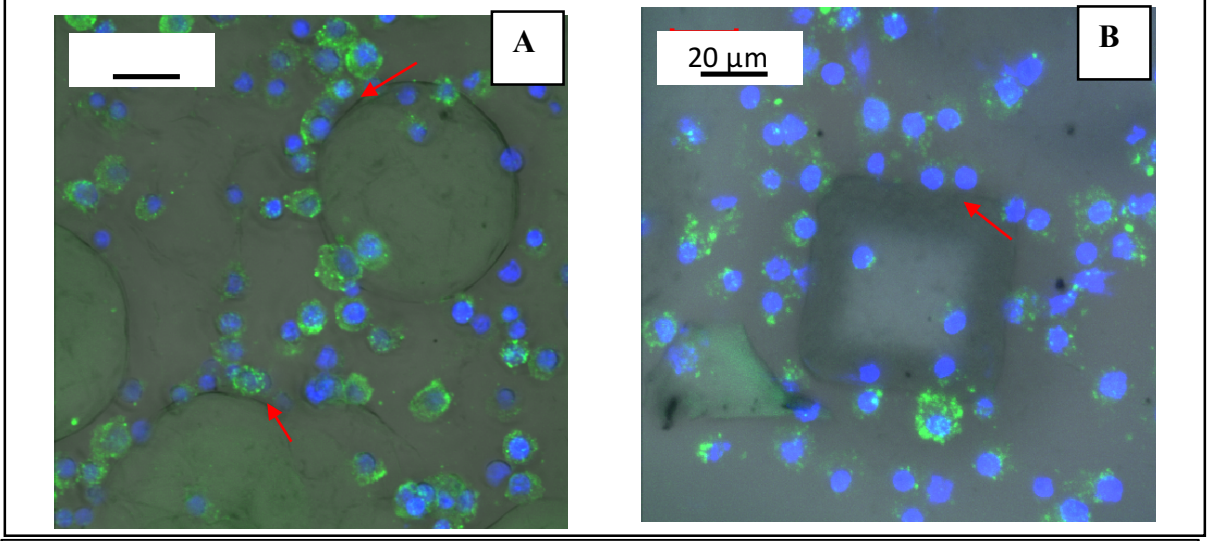

Fig 16: Cell location on posts of **A)** 50 µm circle **B)** 50 µm square patterned films.

4.0 CONCLUSION AND FUTURE DIRECTIONS

We have developed micropatterned polymeric films of various shapes and sizes as a platform for sustained release of drugs. The ability to obtain micropatterned structures on film made of GRAS polymers makes it a versatile delivery system. Films were characterized for their thickness, mechanical properties and contact angle- showing that we were able to develop a diverse set of film compositions using this platform. Micropatterned films required more work to be detached from the mucosa - due to increased surface area provided and the roughness i.e empty spaces to which the mucus conformed. In this work, mucoadhesion can be explained by combination of wetting and mechanical theories- where irregularities on micropatterned films improved mucoadhesion compared to plain films and within the diverse compositions, presence of hydrophilic HPMC increased mucoadhesion over other two compositions. Increased mucoadhesion would translate into higher residence time and intimate contact between drug and mucosal surface. It would be interesting to understand mucoadhesion of films in a dynamic environment which accounts for mastication and chewing motions experienced by the mouth.

Moreover, with use of pH-sensitive polymers in micropatterned films, we were able to manipulate the release of doxycycline hyclate. For the first time, reduced oral pH was taken into account while designing dosage form for periodontitis. Formulating

the drug in pH-sensitive micropatterned films can not only increase residence time in the gingival mucosa but also gradually release it near the required site of action i.e periodontal pockets. Future studies will involve improving stability of DOX in the different compositions and further retarding the release from the film possibly upto a month. Also, it would be necessary to perform functional assays like determining zone of inhibition of micropatterned films using bacterial strains that are associated with periodontitis.

Lastly, macrophages seemed to adhere to the films to an extent, achieving predominantly a rounded morphology which was maintained over 24 h. However, there was a considerable reduction in average surface area suggesting acquisition of a particular phenotype. This sets forth the need for checking regulation of M1 (specifically: TNF α and iNOS) and M2 (specifically: Arg1 and IL-4) markers- to give a better understanding of the immune response that these micropatterns can induce.

Interestingly, we were able to correlate the findings of mucoadhesion and cell morphology to the physical characteristics and contact angle of the films. Indeed, 3D micropatterned films along with pH-sensitive polymers are an attractive model for designing sustained release delivery systems for any drug or disease indication. Unlike previous studies, the present study has utilized the concept of micron scale structures for adhesion on biological surfaces, specifically mucus. This work could

help understand how polymeric films developed by pharmaceutical companies can improve their residence time *in vivo* and the different factors responsible for enhancing mucoadhesion. Also, this provides a stepping stone for exploring how sustained release can be achieved locally (near gingiva) during the treatment of globally prevalent periodontitis. Future studies will demonstrate the kind of immune response elicited by micropattern structures on the film.

APPENDIX

Term	Abbreviation
GIT	Gastro-intestinal Tract
MDDS	Mucoadhesive Drug Delivery Systems
API	Active Pharmaceutical Ingredient
SR	Sustained Release
PDMS	Polydimethylsiloxane
SRP	Scaling and Root Planning
DOX	Doxycycline Hyclate
GRAS	Generally Recognized As Safe
HPMC	Hydroxy Propyl Methyl Cellulose
PEG	Polyethylene Glycol
SEM	Scanning Electron Micrsocopy
UTS	Ultimate Tensile Strength
PDF	Peak Detachment Force
SFS	Salivary Fluid Simulant
DMEM	Dulbecco's Modified Eagle's Medium

BIBLIOGRAPHY

1] Agha-Hosseini, F., et al. (2007). "Stimulated whole salivary flow rate and composition in menopausal women with oral dryness feeling." Oral Dis **13**(3): 320-323.

2] Ali, M. F. and S. Bakalis (2011). "Mucoadhesive polymers for food formulations." Procedia Food Science **1**: 68-75.

3] Anonymous (2001). "Treatment of plaque-induced gingivitis, chronic periodontitis, and other clinical conditions." J Periodontol **72**(12): 1790-1800.

4] Baliga, S., et al. (2013). "Salivary pH: A diagnostic biomarker." J Indian Soc Periodontol **17**(4): 461-465.

5] Bernkop-Schnurch, A. (2005). "Mucoadhesive systems in oral drug delivery." Drug Discov Today Technol **2**(1): 83-87.

6] Bilensoy, E., et al. (2007). "Thermosensitive mucoadhesive gel formulation loaded with 5-Fu: cyclodextrin complex for HPV-induced cervical cancer." Journal of Inclusion Phenomena and Macrocyclic Chemistry **57**(1-4): 363-370.

7] Boddupalli, B. M., et al. (2010). "Mucoadhesive drug delivery system: An overview." J Adv Pharm Technol Res **1**(4): 381-387.

8] Boegh, M. and H. M. Nielsen (2015). "Mucus as a Barrier to Drug Delivery - Understanding and Mimicking the Barrier Properties." Basic & Clinical Pharmacology & Toxicology **116**(3): 179-186.

9] Bromberg, L. E., et al. (2000). "Sustained release of silver from periodontal wafers for treatment of periodontitis." J Control Release **68**(1): 63-72.

10] Buselli, E., et al. (2010). "Evaluation of friction enhancement through soft polymer micro-patterns in active capsule endoscopy." Measurement Science and Technology **21**(10).

11] Champion, J. A., et al. (2008). "Role of particle size in phagocytosis of polymeric microspheres." Pharm Res **25**(8): 1815-1821.

12] Chen, S., et al. (2010). "Characterization of topographical effects on macrophage behavior in a foreign body response model." Biomaterials **31**(13): 3479-3491.

13] Chiang-Hanisko, L., et al. (2014). "[Polypharmacy issues in older adults]." Hu Li Za Zhi **61**(3): 97-104.

14] Chirra, H. D. and T. A. Desai (2012). "Emerging microtechnologies for the development of oral drug delivery devices." Adv Drug Deliv Rev **64**(14): 1569-1578.

15] Da Rocha, H. A., et al. (2015). "Local Drug Delivery Systems in the Treatment of Periodontitis: A Literature Review." J Int Acad Periodontol **17**(3): 82-90.

16] Dodou, D., et al. (2007). "Mucoadhesive micropatterns for enhanced grip." Conf Proc IEEE Eng Med Biol Soc **2007**: 1457-1462.

17] Dowling, D. P., et al. (2011). "Effect of surface wettability and topography on the adhesion of osteosarcoma cells on plasma-modified polystyrene." J Biomater Appl **26**(3): 327-347.

18] Duffo, G. S. and E. Q. Castillo (2004). "Development of an artificial saliva solution for studying the corrosion behavior of dental alloys." Corrosion **60**(6): 594-602.

19] Eaimtrakarn, S., et al. (2001). "Retention and transit of intestinal mucoadhesive films in rat small intestine." Int J Pharm **224**(1-2): 61-67.

20] Eke, P. I., et al. (2012). "Prevalence of Periodontitis in Adults in the United States: 2009 and 2010." Journal of Dental Research **91**(10): 914-920.

21] El-Kamel, A. H., et al. (2007). "Micromatricial metronidazole benzoate film as a local mucoadhesive delivery system for treatment of periodontal diseases." Aaps Pharmscitech **8**(3).

22] Fereol, S., et al. (2006). "Sensitivity of alveolar macrophages to substrate mechanical and adhesive properties." Cell Motil Cytoskeleton **63**(6): 321-340.

23] Fischer, K. E., et al. (2009). "Biomimetic nanowire coatings for next generation adhesive drug delivery systems." Nano Lett **9**(2): 716-720.

24] Fox, C. B., et al. (2015). "Micro/nanofabricated platforms for oral drug delivery." J Control Release **219**: 431-444.

25] Galgut, P. N. (2001). "The relevance of pH to gingivitis and periodontitis." J Int Acad Periodontol **3**(3): 61-67.

26] Gandhi, R. B. and J. R. Robinson (1994). "Oral Cavity as a Site for Bioadhesive Drug-Delivery." Advanced drug delivery reviews **13**(1-2): 43-74.

27] Gilhotra, R. M., et al. (2014). "A clinical perspective on mucoadhesive buccal drug delivery systems." J Biomed Res **28**(2): 81-97.

28] Hickman, G. J., et al. (2016). "The Importance and Clinical Relevance of Surfaces in Tissue Culture." Acs Biomaterials Science & Engineering **2**(2): 152-164.

29] Hua, S., et al. (2015). "Advances in oral nano-delivery systems for colon targeted drug delivery in inflammatory bowel disease: selective targeting to diseased versus healthy tissue." Nanomedicine **11**(5): 1117-1132.

30] Hubbell, J. A., et al. (2009). "Materials engineering for immunomodulation." Nature **462**(7272): 449-460.

31] Irache, J. M., et al. (1996). "Bioadhesion of lectin-latex conjugates to rat intestinal mucosa." Pharm Res **13**(11): 1716-1719.

32] Kapoor, A., et al. (2012). "Systemic antibiotic therapy in periodontics." Dent Res J (Isfahan) **9**(5): 505-515.

33] Koumans, E. H., et al. (2007). "The prevalence of bacterial vaginosis in the United States, 2001-2004; associations with symptoms, sexual behaviors, and reproductive health." Sex Transm Dis **34**(11): 864-869.

34] Lai, S. K., et al. (2009). "Mucus-penetrating nanoparticles for drug and gene delivery to mucosal tissues." Adv Drug Deliv Rev **61**(2): 158-171.

35] Lee, H. S., et al. (2013). "Correlating macrophage morphology and cytokine production resulting from biomaterial contact." J Biomed Mater Res A **101**(1): 203-212.

36] Lehr, C. M., et al. (1992). "Bioadhesion by means of specific binding of tomato lectin." Pharm Res **9**(4): 547-553.

37] Lensen, M. C., et al. (2008). "Cellular responses to novel, micropatterned biomaterials." Pure and Applied Chemistry **80**(11): 2479-2487.

38] Litt, M. (1984). "Comparative studies of mucus and mucin physicochemistry." Ciba Found Symp **109**: 196-211.

39] Loesche, W. J. (1996). Microbiology of Dental Decay and Periodontal Disease. Medical Microbiology. S. Baron. Galveston (TX).

40] Mahdavi, A., et al. (2008). "A biodegradable and biocompatible gecko-inspired tissue adhesive." Proc Natl Acad Sci U S A **105**(7): 2307-2312.

41] Majithiya, R. J., et al. (2006). "Thermoreversible-mucoadhesive gel for nasal delivery of sumatriptan." Aaps Pharmscitech **7**(3): 67.

42] Marsh, P. D. (2010). "Microbiology of dental plaque biofilms and their role in oral health and caries." Dent Clin North Am **54**(3): 441-454.

43] Mason, S. E., et al. (2011). "Stability and bioactivity of tetracycline hydrochloride water medication in a swine production unit." Journal of Swine Health and Production **19**(2): 107-111.

44] McWhorter, F. Y., et al. (2015). "Physical and mechanical regulation of macrophage phenotype and function." Cellular and Molecular Life Sciences **72**(7): 1303-1316.

45] McWhorter, F. Y., et al. (2013). "Modulation of macrophage phenotype by cell shape." Proc Natl Acad Sci U S A **110**(43): 17253-17258.

46] Mishra, R., et al. (2017). "Mucoadhesive vaginal film of fluconazole using cross-linked chitosan and pectin." Journal of Thermal Analysis and Calorimetry.

47] Mohammed-Ali, M. (2012). "Stability study of tetracycline drug in acidic and alkaline solutions by colorimetric method." Journal of Chemical and Pharmaceutical Research **4**(2): 1319-1326

48] Moore, W. E., et al. (1991). "The microflora of periodontal sites showing active destructive progression." J Clin Periodontol **18**(10): 729-739.

49] Mustata, G. and S. M. Dinh (2006). "Approaches to oral drug delivery for challenging molecules." Crit Rev Ther Drug Carrier Syst **23**(2): 111-135.

50] Nair, S. C. and K. R. Anoop (2012). "Intraperiodontal pocket: An ideal route for local antimicrobial drug delivery." J Adv Pharm Technol Res **3**(1): 9-15.

51] Naz, K., et al. (2017). "Formulation and In Vitro Characterization of Thiolated Buccoadhesive Film of Fluconazole." Aaps Pharmscitech **18**(4): 1043-1055.

52] Palacio, M. L. and B. Bhushan (2012). "Bioadhesion: a review of concepts and applications." Philos Trans A Math Phys Eng Sci **370**(1967): 2321-2347.

53] Patel, N. R., et al. (2012). "Cell elasticity determines macrophage function." PLoS One **7**(9): e41024.

54] Paul, N. E., et al. (2008). "Topographical control of human macrophages by a regularly microstructured polyvinylidene fluoride surface." Biomaterials **29**(30): 4056-4064.

55] Peppas, N. A. and J. J. Sahlin (1996). "Hydrogels as mucoadhesive and bioadhesive materials: A review." Biomaterials **17**(16): 1553-1561.

56] Perioli, L., et al. (2004). "Development of mucoadhesive patches for buccal administration of ibuprofen." J Control Release **99**(1): 73-82.

57] Prakasam, A., et al. (2012). "Antibiotics in the management of aggressive periodontitis." J Pharm Bioallied Sci **4**(Suppl 2): S252-255.

58] Prasad, M., et al. (2002). "Measurement of Young's modulus of clay minerals using atomic force acoustic microscopy." Geophysical Research Letters **29**(8).

59] Ramineni, S. K., et al. (2013). "Competing Properties of Mucoadhesive Films Designed for Localized Delivery of Imiquimod." Biomater Sci **1**(7): 753-762.

60] Schutte, R. J., et al. (2009). "In vivo cytokine-associated responses to biomaterials." Biomaterials **30**(2): 160-168.

61] Slots, J., et al. (2004). "Systemic antibiotics in periodontics." J Periodontol **75**(11): 1553-1565.

62] Smart, J. D. (2005). "The basics and underlying mechanisms of mucoadhesion." Adv Drug Deliv Rev **57**(11): 1556-1568.

63] Solheim, E., et al. (2000). "Biocompatibility and effect on osteogenesis of poly(ortho ester) compared to poly(DL-lactic acid)." J Biomed Mater Res **49**(2): 257-263.

64] Sosnik, A., et al. (2014). "Mucoadhesive polymers in the design of nano-drug delivery systems for administration by non-parenteral routes: A review." Progress in Polymer Science **39**(12): 2030-2075.

65] Srivastava, K., et al. (2013). "Impact of reducing dosing frequency on adherence to oral therapies: a literature review and meta-analysis." Patient Prefer Adherence **7**: 419-434.

66] Stachelek, S. J., et al. (2011). "The effect of CD47 modified polymer surfaces on inflammatory cell attachment and activation." Biomaterials **32**(19): 4317-4326.

67] Szymanska, E., et al. (2014). "Vaginal Chitosan Tablets with Clotrimazole-Design and Evaluation of Mucoadhesive Properties Using Porcine Vaginal Mucosa, Mucin and Gelatine." Chemical & Pharmaceutical Bulletin **62**(2): 160-167.

68] Takahashi, N., et al. (1997). "Acid tolerance and acid-neutralizing activity of Porphyromonas gingivalis, Prevotella intermedia and Fusobacterium nucleatum." Oral Microbiol Immunol **12**(6): 323-328.

69] Takahashi, N. and C. F. Schachtele (1990). "Effect of pH on the growth and proteolytic activity of Porphyromonas gingivalis and Bacteroides intermedius." J Dent Res **69**(6): 1266-1269.

70] Takebe, J., et al. (2003). "Titanium surface topography alters cell shape and modulates bone morphogenetic protein 2 expression in the J774A.1 macrophage cell line." J Biomed Mater Res A **64**(2): 207-216.

71] Tejada, G., et al. (2017). "Development and Evaluation of Buccal Films Based on Chitosan for the Potential Treatment of Oral Candidiasis." Aaps Pharmscitech **18**(4): 936-946.

72] Traverso, G., et al. (2015). "Microneedles for drug delivery via the gastrointestinal tract." J Pharm Sci **104**(2): 362-367.

73] Varum, F. J., et al. (2012). "Mucus thickness in the gastrointestinal tract of laboratory animals." J Pharm Pharmacol **64**(2): 218-227.

74] Wilson, J. (2004). "Managing recurrent bacterial vaginosis." Sex Transm Infect **80**(1): 8-11.

75] Wong, C. F., et al. (1999). "An in-vitro method for buccal adhesion studies: importance of instrument variables." Int J Pharm **180**(1): 47-57.

76] Wu, Y. and R. Fassihi (2005). "Stability of metronidazole, tetracycline HCl and famotidine alone and in combination." Int J Pharm **290**(1-2): 1-13.

77] Yamamoto, M., et al. (2015). "Theoretical Explanation of the Lotus Effect: Superhydrophobic Property Changes by Removal of Nanostructures from the Surface of a Lotus Leaf." Langmuir **31**(26): 7355-7363.

78] Zhang, H., et al. (2014). "Mucus as a Barrier for Biopharmaceuticals and Drug Delivery Systems." 59-97.